ARCHIVES OF ACOUSTICS
4, 4, 289-304 (1979)

OBJECTIVE ACOUSTICAL METHODS IN PHONIATRIC DIAGNOSTICS OF SPEECH ORGAN DISORDERS*

JANUSZ KACPROWSKI

Institute of Fundamental Technological Research,
Polish Academy of Sciences (00-049 Warszawa, ul. Świętokrzyska 21)

Physical parameters of the speech signal contain essential information on the anatomical structure and the kinematics of the biological sound source, i.e. the human speech organ. Several objective acoustical methods have been proposed and developed recently, which not only assist, but in some cases are even superior to the classical, mostly intrusive and/or subjective diagnostic methods, commonly used at present in clinical practice in laryngology and phoniatrics.

The subject of the present paper is the theoretical fundamentals and the engineering performance of some selected methods and systems for speech signal processing and analysis, aimed at acoustical diagnosis of larynx and vocal tract pathology. The current status of fundamental research in this domain is briefly reviewed and discussed, including the scientific activity and achievements of the Department of Cybernetic Acoustics, IFTR – PAS. Preliminary results of experimental research are given. Special attention is paid to the role of model investigations in the development of acoustical diagnostic methods and systems in laryngology and phoniatrics. The references play a role of the reader's guide throughout the rather scarce literature on the subject considered.

1. Introduction

For years physicians have used two traditional methods for the examination of speech organ disorders and pathology. The first method relies on the subjective auditory evaluation of the qualities of the patient's voice. The second method consists in visual observation of the articulatory effectors using more or less complex techniques, such as direct or indirect laryngoscopy, laryngeal stroboscopy etc. The principal handicap of the auditory methods is their subjectivity and the lack of absolute quantitative standards, although many attempts have been made to qualify and to quantify the subjective

* This paper was written under the nodal research problem 10.4 "The nervous system and biocybernetic systems and elements".

measurements of voice quality defects (cf. PERKINS [29]). The main shortcoming of the visual methods is that they are as a rule uncomfortable, and sometimes even painful to the patient, being besides ineffective for early detection of pathology. Consequently, their application is usually confined to diagnosis during the later stages of the disease and to surgical situations. More advanced techniques, such as high-speed motion picture analysis, glottography, electromyography, pneumatachography etc. have mostly research applications.

New objective methods in phoniatric diagnostics became feasible in the early sixties of this century, when FANT [4] presented his acoustical theory of speech production and FLANAGAN [8] summarized the recent results of speech communication research in his book on speech analysis, synthesis and perception. Since then the speech signal has been considered — from a physical point of view — as the output of the concatenation of three independent acoustical filters, which represent the glottal source, the vocal tract and the mouth and/or nose radiation impedance, respectively. Moreover, the advanced computer technique has offered new conspicuous facilities in speech signal processing and analysis. Consequently, the research work in the new field of applied acoustics, viz. the acoustical diagnostics of speech organ disorders, was initiated and has been henceforth intensively developed, offering many possibilities of practical applications not only in the medicine: laryngology and phoniatrics, but also in acoustic phonetics, applied linguistics and even in vocalistics.

2. General characteristics of acoustical methods

Acoustical diagnostic methods in laryngology and phoniatrics, which are based — generally speaking — on an analysis of the information content of the speech signal as the final and natural output of the speech organ, have recently been applied in clinical practice [30-35]. They not only support, but in some cases are even superior to the conventional methods, since

— they are used under normal conditions of phonation and articulation;

— they neither need any surgical tool nor foreign substance to be introduced into the patient's body, nor have to be aided by any painful and dangerous intrusive procedure;

— they enable the real-time visualization of the acoustic parameters of the speech signal on the TV monitor, computer display or other conventional peripheral device of a computer system, and are thus especially convenient during rehabilitation process, since the loss of hearing, usually associated with speech disorders, may be compensated by the additional and auxiliary information channel of the sight organ;

— the printed output of the computer-aided analysis of the speech signal may be inserted into the patient's medical history and used afterwards for the objective evaluation of the effectiveness of the therapy.

Acoustical methods consist in the measurement and analysis of those physical parameters of the speech signal which are tightly correlated with the anatomical structure and with the kinematics of the biological source, i.e. the human speech organ. The development and application of these methods in clinical practice must be based on the understanding of the acoustics of speech production and supported by the knowledge of versatile and universal physical models of the biological system under consideration, i.e. the larynx source and the vocal tract. In fact, modelling offers the best means of getting an insight into the functional relations between the acoustical parameters of the speech signal and the intrinsic structural and kinematic features of the speech organ under both normal and pathological conditions.

The directly measurable diagnostic signal is the acoustic pressure $p(t)$ of the speech wave at a definite point on the symmetry axis of the subject's mouth. This signal may be considered, at least during the articulation of voiced speech sounds with glottal excitation, as the response of a linear and passive transmission system which represents the vocal tract and is described by its transfer function $H(s)$, being submitted to the action of the impulse excitation function of the larynx source, i.e. the volume velocity $U_g(s)$ of air in the glottis and loaded by the radiation impedance $Z_r(s)$. These relations are schematically shown in Fig. 1.

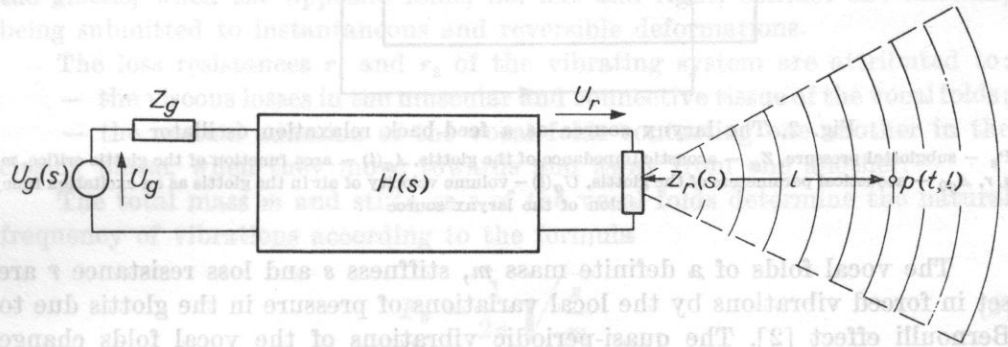

Fig. 1. Equivalent electrical circuit of the speech organ during the articulation of voiced speech sounds with glottal excitation

$U_g(s)$ – excitation function of the larynx source, Z_g – internal impedance of the larynx source, U_g – volume velocity of air in the glottis, U_r – volume velocity of air in the mouth orifice, $H(s)$ – transfer function of the vocal tract, $Z_r(s)$ – radiation impedance of the mouth orifice, $p(t, l)$ – acoustic pressure of the speech wave in the measurement point at a distance l on the symmetry axis of the mouth

The well known general expression for the sound pressure $P(s)$ of the speech wave in Laplace transform presentation according to [4] is given by the equation

$$P(s) = \mathcal{L}\{p(t)\} = U_g(s)H(s)Z_r(s), \tag{1}$$

where Z_r stands for the radiation impedance of the mouth outlet orifice, usually approximated as a circular vibrating piston set in a spherical or infinite flat baffle which simulates the human head [8].

It is evident from (1) that the speech wave reflects the intrinsic features of both the larynx source and the vocal tract. This fact is very promising from the point of view of further diagnostic applications, since the laryngeal pathology and the anomalies of the vocal tract constitute the majority of speech organ disorders most frequently occurring in clinical practice.

3. Physical models of the larynx source

According to the myoelastic-aerodynamic theory formulated by van den BERG [1], the human larynx is – from a physical point of view – a relaxation feed-back oscillator whose output, i.e. the flow or volume velocity $U_g(t)$ of air in the glottis, affects the internal parameters of the system, including those which determine the glottis impedance Z_g. These relations are illustrated schematically in the block diagram shown in Fig. 2.

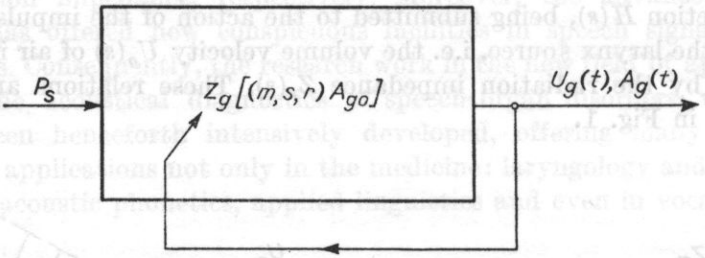

Fig. 2. The larynx source as a feed-back relaxation oscillator

P_s – subglottal pressure, Z_g – acoustic impedance of the glottis, $A_g(t)$ – area function of the glottis orifice, m, s, r, A_{g0} – acoustical parameters of the glottis, $U_g(t)$ – volume velocity of air in the glottis as an excitation function of the larynx source

The vocal folds of a definite mass m, stiffness s and loss resistance r are set in forced vibrations by the local variations of pressure in the glottis due to Bernoulli effect [2]. The quasi-periodic vibrations of the vocal folds change the acoustic impedance Z_g of the glottis and thus modulate the air flow $U_g(t)$ which at the entrance to the vocal tract has the form of recurrent discrete triangle shaped pulses. The latter play the role of an impulse source function $U_g(t)$ which excites vibrations of air in the vocal tract at frequencies corresponding to the resonances of the vocal-tract cavities.

The mechanical vibrating system of the vocal folds may be modelled in many ways [18], starting with the simplest single – mass model with lumped constants and one degree of freedom elaborated by FLANAGAN and LANDGRAF [10], up to complex models with distributed constants composed of elementary masses, stiffnesses and loss resistances, as proposed by ISHIZAKA [15]. Such a sophisticated model is, however, neither necessary nor even convenient in medical diagnostics, since the main physiological features of the human larynx

may be simulated with sufficient accuracy in the two-mass model with lumped constants, proposed by ISHIZAKA and MATSUIDARA [16], presented by FLANAGAN [9] to the 7th ICA Congress in Budapest and described in details by ISHIZAKA and FLANAGAN [17].

In the latter model each vocal fold, left and right, is divided into two partial masses m_1 and m_2 which represent its lower and upper parts, respectively. The masses m_1 and m_2 are mutually coupled by the spring s_c which represents the bending stiffness of the vocal folds in the vertical plane parallel to the direction of vibrations. In this way the two-mass model simulates an essential physiological feature of the biological system,. i.e. the deformability of the vocal folds and the phase difference between the displacements of their lower and upper edges in quasi-harmonic motion. The ratio at which the total mass of each vocal fold is divided into its partial components m_1 and m_2, may vary widely depending on the realistic physiological or pathological conditions.

The springs s_1 and s_2 associated with the masses m_1 and m_2 represent the individual non-linear stiffnesses of both parts of each vocal fold, i.e. the lower m_1 and the upper m_2 which are opposed to:

– the momentary displacements of the masses m_1 and m_2 from their neutral positions;

– the viscoelastic deformations of the vocal folds in the closing phase of the glottis, when the opposite folds, i.e. left and right, contact one another, being submitted to instantaneous and reversible deformations.

The loss resistances r_1 and r_2 of the vibrating system are attributed to:

– the viscous losses in the muscular and connective tissue of the vocal folds;

– the mutual adhesion of the vocal folds contacting one another in the closing phase, when they move towards and away from one another.

The total mass m and stiffness s of the vocal folds determine the natural frequency of vibrations according to the formula

$$F_0 = \frac{1}{2\pi}\sqrt{\frac{s}{m}}. \tag{2}$$

Under real conditions of phonation and articulation, due to the contraction of the vocalis muscles, the vocal folds are shortened or elongated and their tension Q varies to a limited extent. Their mass m and stiffness s also vary and the pitch or larynx tone frequency changes from the value F_0 given by (2) to the value F_0^1 expressed as follows:

$$F_0^1 = \frac{1}{2\pi}\sqrt{\frac{sQ}{m/Q}} = QF_0. \tag{3}$$

The tension coefficient Q is commonly used in model investigations as an additional parameter which determines the real physiopathological behaviour of the subject's larynx source.

It is evident from this brief description that the two-mass model of the human larynx is versatile enough to take into account and to reflect not only in qualitative, but also in quantitative terms, several laryngeal disorders and anomalies most frequently occurring in clinical practice. The following examples may be quoted. Benign growths, such as vocal nodules and polyps located on one or both folds, increase their mass, whereas the partial atrophy of the vocal fold is equivalent to the reduction of its effective mass. The immobility of one or both vocal folds due to unilateral or bilateral recurrent laryngeal palsy (paralysis) may be expressed in terms of their stiffness value which approaches infinity in spastic cases and reduces to zero in paretic cases.

4. Objective evaluation of laryngeal pathology

It is evident from (1) that the acoustic measures of laryngeal pathology, based on the analysis of the speech wave form $p(t)$, are affected by the vocal tract structure $H(s)$ which, especially at an early stage of pathological development, may distort or even mask some of the important acoustical attributes of larynx disorder. The technique of inverse filtering of speech may be used to remove the influence of the supraglottal structure upon the speech wave form $p(t)$ and to obtain the residue signal whose characteristics are correlated with the movements of the vocal folds only, as it was proposed by MILLER [26]. Thus, if the speech signal contains acoustical information indicative of laryngeal pathology, the measures based on the residue signal should be as informative as the original speech signal itself, if not more so. Valuable information concerning the application of inverse filtering of speech for detecting and evaluating laryngeal pathology may be found in the works of DAVIS [3], KOIKE and MARKEL [22], and MARKEL and GRAY [23].

If the speech signal expressed by (1) is submitted to pre-emphasis equivalent to the reciprocal of the mouth radiation factor $Z_r(s)$ and if an inverse filter is used whose reciprocal is an estimate of the vocal tract transfer function $H(s)$, the result of inverse filtering is the residue signal which is associated with the larynx source excitation function $U_g(s)$ only.

For normal voice, the residue signal has the form of a series of sharp spikes at the initiation of the successive pitch periods T_0, with an irregular or noisy behaviour of relatively low amplitudes between the spikes. The cyclic oscillations within the pitch periods of the primary speech signal have been effectively removed by inverse filtering. The noisy component in the residue signal decays so that during the other half of each pitch period it is much smaller than the spikes at the pitch period initiation. The most important feature of the residue signal for normal voices is thus a high peak signal to noise ratio within the other half of each pitch period.

In pathological cases, on the other hand, especially when an incomplete glottal closure occurs, the assumption of vocal tract and larynx source separa-

bility in the linear model of speech production is not valid. As a rule, the more severe the pathology is, the less distinct pattern of periodic spikes can be observed in the residue signal. In an extremely severe case of vocal fold fixation, the acoustic wave form contains a small, if any, periodic component. In the residue signal the cyclic behaviour has been completely eliminated, leaving a very noisy nonperiodic signal. The residue signals of a normal and two pathological voices are shown in Fig. 3, after KOIKE and MARKEL [22], and MARKEL and GRAY [23].

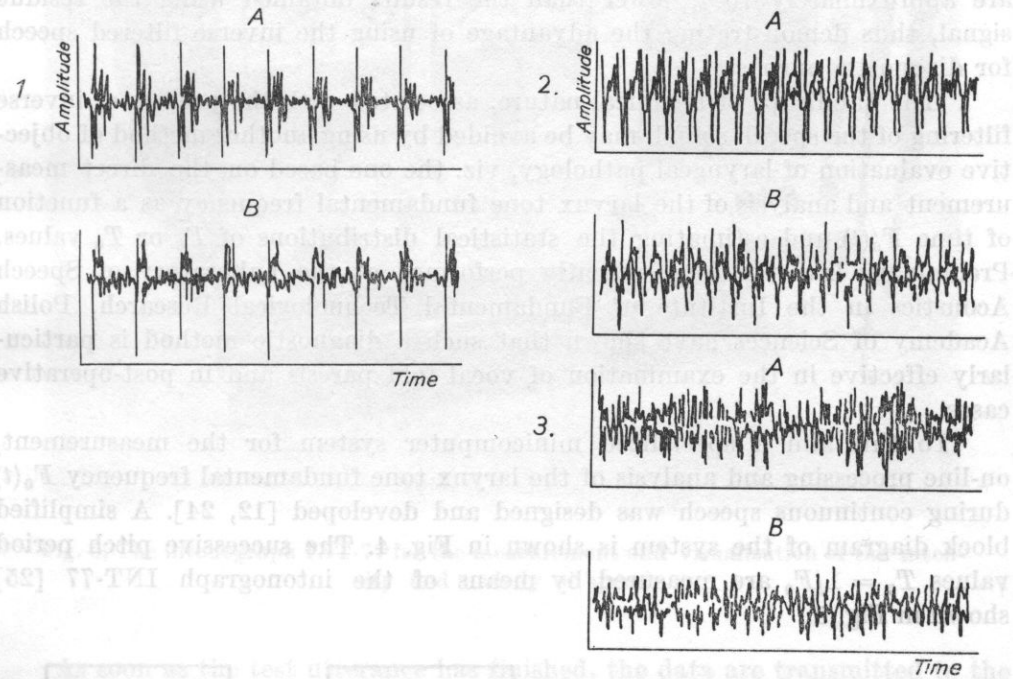

Fig. 3. Examples of the original (A) and residual (B) speech signals of a normal voice (1) and of two pathological voices: with a small vocal nodule (2) and with an advanced laryngeal cancer (3), after [22, 23]

Thus the acoustic features extracted from the residue signal may have potentially high value for the objective evaluation of the abnormal vocal fold vibrations as a common effect of laryngeal pathology. In a recent study by DAVIS [3], the six features which describe the acoustical structure of the speech signal $p(t)$ previously submitted to inverse filtering, are the following:

- the pitch amplitude of the residue signal, PA;
- the pitch period perturbation quotient, PPQ;
- the pitch amplitude perturbation quotient, APQ;
- the coefficient of excess, EX;
- the spectral flatness of the inverse filter, SFF;
- the spectral flatness of the residue signal, SFR.

These measures were then separately and jointly analyzed for their effectiveness in discriminating between normal and pathological voices. In a closed maximum likelihood test using sustained vowel sounds from 17 normal and 21 pathological speakers, each single feature successfully discriminates between 65 % and 85 % of normal and pathological sounds. The six features jointly produce a 95 % probability of detection for the pathological sounds and a 6 % probability of false alarm for the normal sounds. An analogous joint discrimination test using the unprocessed vowel sounds gave results which are approximately 10 % lower than the results obtained using the residue signal, thus demonstrating the advantage of using the inverse filtered speech for diagnostic purposes.

The handicaps of technical nature, associated with the process of inverse filtering of the speech signal, may be avoided by using another method of objective evaluation of laryngeal pathology, viz. the one based on the direct measurement and analysis of the larynx tone fundamental frequency as a function of time $F_0(t)$ and estimating the statistical distributions of F_0 or T_0 values. Preliminary investigations, recently performed at the Laboratory of Speech Acoustics in the Institute of Fundamental Technological Research, Polish Academy of Sciences have shown that such a diagnostic method is particularly effective in the examination of vocal fold paresis and in post-operative cases.

To this aim a specialized minicomputer system for the measurement, on-line processing and analysis of the larynx tone fundamental frequency $F_0(t)$ during continuous speech was designed and developed [12, 24]. A simplified block diagram of the system is shown in Fig. 4. The successive pitch period values $T_0 = 1/F_0$ are measured by means of the intonograph INT-77 [25] shown in Fig. 5.

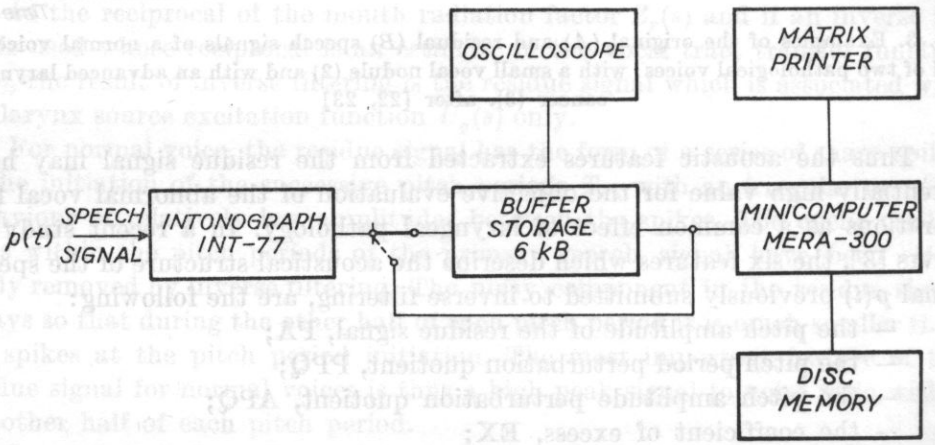

Fig. 4. Block diagram of the minicomputer system for the measurement and analysis of the fundamental frequency and the pitch period of the larynx source, after [12, 24]

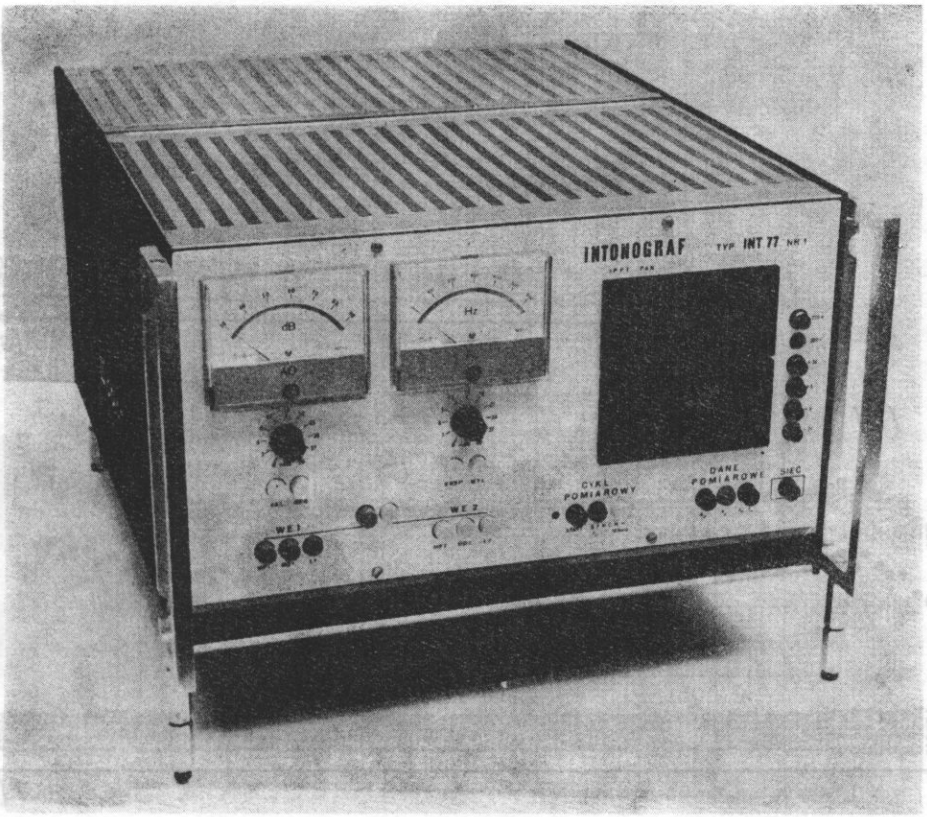

Fig. 5. The intonograph INT-77 for the measurement and visualization of the intensity and melody of speech

As soon as the test utterance has finished, the data are transmitted to the minicomputer MERA-304 for further processing and analysis, according to special software procedures. The phonetic material consists of standard sentences, both affirmative and interrogative, and of a newspaper text of 1 minute duration. The analyzed speech signal contains as a whole about 6000 samples of T_0 or F_0 values and is thus long enough to be considered as a stationary ergodic process.

Two kinds of criteria for the objective evaluation of laryngeal pathology have been accepted. The first measure is the irregularity of the intonation curve $F_0(t)$, which appears chiefly within the final parts of interrogative sentences (Fig. 6). The second measure is the statistical distribution of the T_0 or F_0 values, which is computed by the long-term analysis of the speech signal corresponding to the newspaper text. The results of the statistical analysis are presented as printed output of the minicomputer in the form of histograms of the momentary T_0 values and histograms of the momentary incremental

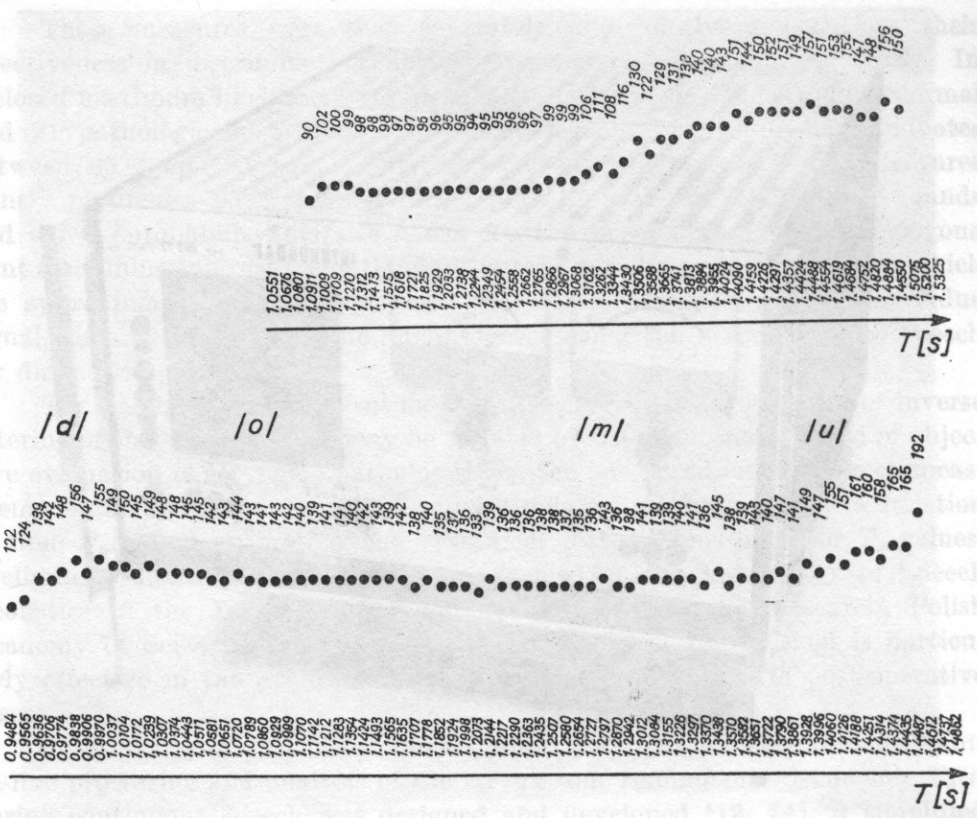

Fig. 6. Fundamental frequency $F_0(t)$ of the larynx tone as a function of time, measured within the final part of an interrogative sentence uttered by a male voice in bilateral vocal fold paralysis, before (lower curve) and after (upper curve) medical treatment [13, 14]

ΔT_0 values in sucessive pitch periods (Fig. 7). The histograms are described by several statistical parameters constituting the quantitative measures of the laryngeal pathology, such as e.g.: mean value $\overline{F}_0$ or $\overline{T}_0$, variance D, standard deviation σ and central moments of the 3rd and 4th order which are used for computing the asymmetry AS and coefficient of excess EX of the T_0 or F_0 distributions [13, 14].

The method was verified under clinical conditions in the Otolaryngological Clinic of the Institute of Surgery, Medical Academy, in Warsaw, on 140 pathological voices with documented larynx disorders. It has been proved that:

— for diagnostic purposes the ΔT_0 distributions are more informative generally, than the T_0 distributions;

— the most effective measures for discriminating between normal and pathological voices are: the asymmetry AS and excess EX of both T_0 and ΔT_0 distributions, as well as the standard deviation σ of the ΔT_0 distribution;

— the inability of a pathological larynx to convey speech melody and

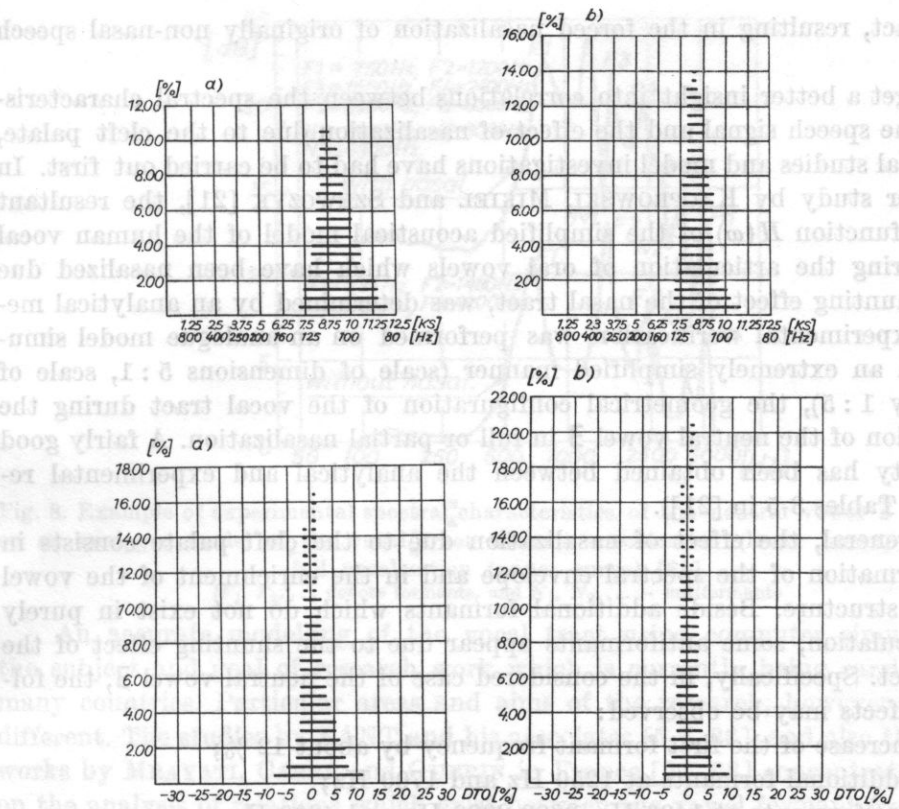

Fig. 7. Examples of printed computer outputs as histograms of the momentary absolute T_0 values (upper part of the figure) and histograms of the relative incremental ΔT_0 values (lower part of the figure) in the case of a male voice with a unilateral vocal fold paralysis after surgical intervention, before (*a*) and after (*b*) rehabilitation

intonation may be effectively evaluated by the analysis of the $F_0(t)$ curve as a function of time within interrogative sentences (cf. Fig. 6).

The results obtained previously are promising and encourage further research. The method and system proposed will hopefully provide facilities for objective computer-aided evaluation of laryngeal pathology in routine clinical practice before and after medical treatement or surgical intervention and during the process of rehabilitation.

5. Objective evaluation of vocal tract pathology

The most frequently occurring pathology of the vocal tract is the cleft palate* (med.: palatoschisis) whose direct effect consists in the permanent and uncontrolled acoustical coupling between the pharynx-mouth cavity and the

* Cleft palate occurs — depending on demographic conditions — in one case for several hundred to one thousand births.

nasal tract, resulting in the forced nasalization of originally non-nasal speech sounds.

To get a better insight into correlations between the spectral characteristics of the speech signal and the effect of nasalization due to the cleft palate, theoretical studies and model investigations have had to be carried out first. In an earlier study by KACPROWSKI, MIKIEL and SZEWCZYK [21], the resultant transfer function $H(\omega)$ of the simplified acoustical model of the human vocal tract during the articulation of oral vowels which have been nasalized due to the shunting effect of the nasal tract, was determined by an analytical method. Experimental verification was performed on an analogue model simulating in an extremely simplified manner (scale of dimensions 5 : 1, scale of frequency 1 : 5), the geometrical configuration of the vocal tract during the articulation of the neutral vowel ∃ in full or partial nasalization. A fairly good conformity has been obtained between the analytical and experimental results (cf. Tables 3-5 in [21]).

In general, the effect of nasalization due to the cleft palate consists in the deformation of the spectral envelope and in the enrichment of the vowel formant structure. Beside additional formants which do not exist in purely oral articulation, some antiformants appear due to the shunting effect of the nasal tract. Specifically, in the considered case of the neutral vowel ∃, the following effects may be observed:

— increase of the first formant frequency by about 12 %;
— additional formants at 1250 Hz and 1700 Hz;
— antiformants at 1400 Hz, 2800-2900 Hz and 4200 Hz;
— disappearance of the second formant $F2$ at a frequency $F_2 = 1500$ Hz due to the appearance of an antiformant at 1400 Hz.

These effects are exemplified by spectral characteristics shown in Fig. 8. The intensity of cleft palate, expressed in terms of a gradual increase of the oral-nasal coupling factor from about 12 % up to its maximal value, affects both the formant-antiformant frequencies and amplitudes, as may be seen in Figs. 10-14 of the previously cited work [21].

The results of our preliminary experiments have confirmed the potential possibility of evaluating the cleft palate by spectral analysis of voiced speech sounds, when using the phonospectroscopic method [30]. The future clinical application of this metod must be based, however, on a better knowledge of a universal articulatory model of the vocal tract, which could be adapted for:

— reproducing the anatomy of the vocal tract during the articulation of sustained oral vowels in all individual variants, depending on the personal features of the patient's voice under both normal and pathological conditions;
— reflecting the losses in the vocal tract and the radiation impedance of the mouth and nose orifices;
— introducing an additional parameter which would express in a quantitative manner the degree of nasalization determined by the extent of cleft palate.

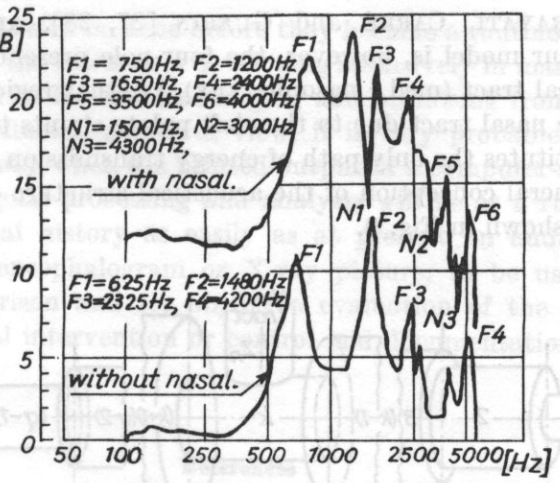

Fig. 8. Example of experimental spectral characteristics of the neutral vowel ∃ measured on an analogue model of the vocal tract without nasalization (lower curve) and with full nasalization (upper curve) [21].
[F_1, F_2,... denote formants, and N_1, N_2,... – antiformants

An accurate modelling of the vocal tract using computer simulation is the subject and goal of research work which is currently being carried on in many countries. Particular areas and aims of the research, however, may be different. The studies by FANT and his associates [5-7, 36], and also the recent works by MRAYATI, CARRÉ and GUERIN in France [27, 28] concentrate mainly on the analysis of relations which exist between the vowel formant frequencies and bandwidths on the one hand, and the acoustical characteristics of the physical model on the other hand, including the boundary effects related to the subglottal system and glottis, losses in the vocal cavity walls and the lip termination. The primary aim of FLANAGAN and co-authors [9-11, 17], on the other hand, has been to develop a working model of the vocal tract and the larynx source for the synthesis of speech in man-machine voice communication systems.

The present state of art in vocal tract modelling and some of the problems involved have recently been discussed in detail by WAKITA and FANT [36]. The conclusion is that much research work must still be done before an improved and standardized model of the vocal tract can be established. In the meantime, however, an approach has been made in the Department of Cybernetic Acoustics, IFTR-PAS, toward a simulative model of the vocal tract including the effect of nasalization due to the cleft palate (cf. KACPROWSKI [19, 20]). The model, which is intended for clinical application in computer-aided acoustical diagnostics in laryngology and phoniatrics, is based on the distributed element transmission line representation of the vocal tract, approximated in the form of a concatenation of n elementary T - type four-poles, as proposed by FLANAGAN [8], and resembles to some extent the recent French model

described by MRAYATI, CARRÉ and GUERIN [27, 28]. An essential feature and novelty of our model is, however, the four-pole presentation of the bifurcation of the vocal tract (med.: nasopharynx), i.e. that region where the input impedance of the nasal tract due to the cleft palate shunts the pharynx-mouth tract which constitutes the only path of energy transmission in purely oral articulation. The general conception of the acoustical structure of the latter model is schematically shown in Fig. 9.

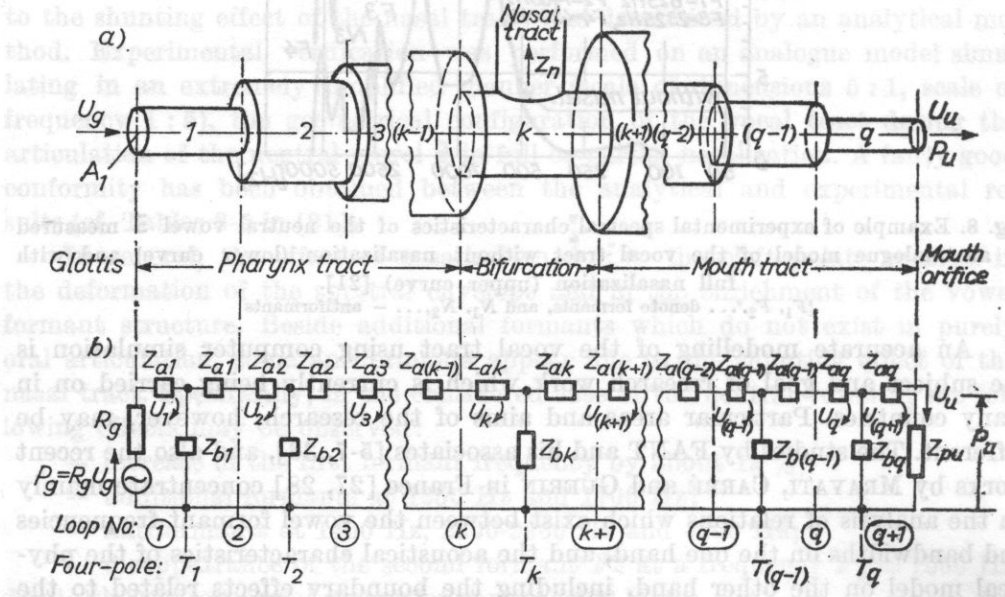

Fig. 9. Acoustical model of the pharynx-mouth vocal tract including the shunting effect of the input impedance Z_n of the nasal tract (*a*) and its equivalent electrical four-pole circuit (*b*) [19]

Since our present interest is the objective evaluation of vocal tract pathology in terms of formant-antiformant frequencies, amplitudes and bandwidths, digital computer simulation of the model will be done in the frequency domain only, in order to allow the frequency resolution up to a few Hz for the sake of accuracy, in the case of sustained voiced speech sounds with glottal excitation.

6. Conclusions

The aim of the present paper has been to indicate the potential possibilities of using acoustical diagnostic methods for objective evaluation of larynx and vocal tract pathology, and to present the actual state of research in this domain. Although some of the experimental methods and systems have recently been applied with success in laryngology and phoniatrics, a great deal

of research work must still be done before they become a routine in clinical practice. Since, however, the research is developing intensively in many countries and the results obtained so far are encouraging and promising from both scientific and practical, i.e. clinical, points of view, it is very probable, if not certain, that the time is coming when the printed output of a computer-aided diagnostic system of speech signal processing and analysis will be as a rule inserted into the patient's medical history as easily as at present an audiogram, electrocardiogram, electroencephalogram or X-ray picture, to be used later on for year-to-year comparison and for objective evaluation of the effectiveness of the therapy, surgical intervention or control and documentation of the rehabilitation process.

References

[1] J. W. van den BERG, *Myoelastic-aerodynamic theory of voice production*, J. Speech Hearing Res., **1**, 227-244 (1959).

[2] J. W. van den BERG, J. T. ZANTEMA, P. DOORNENBAL Jr., *On the air resistance and the Bernoulli effect of the human larynx*, J. Acoust. Soc. Am., **29**, 626-631 (1957).

[3] S. B. DAVIS, *Computer evaluation of laryngeal pathology based on inverse filtering of speech*, Speech Comm. Res. Lab., Monograph No 13, Santa Barbara, California (1976).

[4] G. FANT, *Acoustic theory of speech production*, Mouton and Co., s'-Gravenhage, 1960.

[5] G. FANT, *Vocal tract wall effects, losses and resonance band widths*, STL-QPSR, 2-3, 28-52 (1972).

[6] G. FANT, *Vocal tract area and length perturbations*, STL-QPSR, 4, 1-14 (1975).

[7] G. FANT, L. NORD, P. BRANDERUD, *A note on the vocal tract wall impedance*, STL-QPSR, 4, 13-20 (1976).

[8] J. L. FLANAGAN, *Speech analysis, synthesis and perception*, Springer Verlag, Berlin – Heidelberg – New York, 1st edition 1965, 2nd edition 1972.

[9] J. L. FLANAGAN, *Focal points in speech communication research*, Report 21-G-3, Proc. 7th ICA Congress, Budapest, 1971.

[10] J. L. FLANAGAN, L. L. LANDGRAF, *Self-oscillating source for vocal-tract synthesizers*, IEEE Trans. Audio Electroacoustics, AU-16, 57-64 (1968).

[11] J. L. FLANAGAN, K. ISHIZAKA, K. SHIPLEY, *Synthesis of speech from a dynamic model of the vocal cords and vocal tract*, Bell System Techn. Journal, **54**, 485-506 (1975).

[12] R. GUBRYNOWICZ, W. MIKIEL, P. ŻARNECKI, *Evaluation de l'état pathologique des cordes vocales d'après l'analyse des variations du fondamental*, 8-èmes Journées d'Etudes du Groupe de la Communication Parlée, Vol. 1, 22-27, Institute de Phonétique, Aix-en-Provence, France, 1977.

[13] R. GUBRYNOWICZ, W. MIKIEL, P. ŻARNECKI, *An acoustical method for evaluating the larynx source in the case of vocal folds pathology*, Archives of Acoustics (in print).

[14] R. GUBRYNOWICZ, W. MIKIEL, P. ŻARNECKI, *Acoustical analysis for evaluation of laryngeal disfunction in the case of vocal cord paralysis*, Speech Analysis and Synthesis, Vol. 5, IFTR-PAS, PWN, Warszawa (in press).

[15] K. ISHIZAKA, *On model of the larynx*, J. Acoust. Soc. Am., **22**, 293-294 (1968).

[16] K. ISHIZAKA, M. MATSUIDARA, *What makes the vocal cords vibrate?* Proc. 6th ICA Congress, Report B-1-3, Tokyo 1968.

[17] K. ISHIZAKA, J. L. FLANAGAN, *Synthesis of voiced sounds from a two-mass model of the vocal cords*, Bell System Techn. Journal, **51**, 1233-1268 (1972).

[18] J. KACPROWSKI, *Physical models of the larynx source*, Archives of Acoustics, **2**, 1, 47-70 (1977).

[19] J. KACPROWSKI, *A simulative model of the vocal tract including the effect of nasalization*, Archives of Acoustics, **2**, 4, 235-255 (1977).

[20] J. KACPROWSKI, *An acoustical model of the vocal tract for diagnostics of cleft palate*, Speech Analysis and Synthesis, Vol. 5, IFTR-PAS, PWN Warszawa (in print).

[21] J. KACPROWSKI, W. MIKIEL, A. SZEWCZYK, *Acoustical modelling of cleft palate*, Archives of Acoustics, **1**, 2, 137-158 (1976).

[22] Y. KOIKE, J. D. MARKEL, *Application of inverse filtering for detecting laryngeal pathology*, Annals Otol. Rhinol. Laryngol., **84**, 117-124 (1975).

[23] J. D. MARKEL, A.H. GRAY, *Linear prediction of speech*, Springer Verlag, Berlin-Heidelberg-New York 1976.

[24] W. MIKIEL, P. ŻARNECKI, *A computer system for measuring and processing of acoustical data*, Proc. XXIII Open Seminar on Acoustics, Polish Acoust. Soc., 70-72, Wisła 1976 (in Polish, abstract in English).

[25] W. MIKIEL, R. GUBRYNOWICZ, W. HAGMAJER, *Intonograph — a system for measuring and visualization of the intensity and melody of speech*, Proc. XXIX Open Seminar on Acoustics Polish Acoust. Soc., 120-124, Gdańsk—Władysławowo 1977 (in Polish, abstract in English).

[26] R. L. MILLER, *Nature of the vocal cord wave*, J. Acoust. Soc. Am., **31**, 667-677 (1959).

[27] M. MRAYATI, R. CARRÉ, *Relations entre la forme du conduit vocal et les caractéristiques acoustiques des voyelles françaises*, E.N.S. d'Électronique et de Radioéléctricité de Grenoble (unpublished report), 1975.

[28] M. MRAYATI, B. GUERIN, *Études des caractéristiques acoustiques des voyelles françaises par simulation du conduit vocal avec pertes*, Revue d'Acoustique, **9**, 36, 18-32 (1976).

[29] W. H. PERKINS, *Vocal function: a behavioural analysis*, Handbook of Speech Pathology and Audiology, Appleton Century Croft, New York 1971.

[30] W. TŁUCHOWSKI, W. MIKIEL, A. KOMOROWSKA, E. WIDLICKA, *An approach to the correlation of bioelectric and phonospectroscopic investigations in different types of cleft palate operations in children*, Otolaryngologia Polska, **28**, 6a, 70-77 (1974) (in Polish, abstract in English).

[31] W. TŁUCHOWSKI, W. MIKIEL, A. NIEDŹWIECKI, A. KOMOROWSKA, *Phonospectroscopic investigations in one-sided and two-sided paresis of laryngeal nerves*, Diary of the 29th Meeting of Polish Oto-Laryngologists, Białystok 1974, 359-363 (in Polish).

[32] W. TŁUCHOWSKI, J. KACPROWSKI, W. MIKIEL, A. NIEDŹWIECKI, A. KOMOROWSKA, *Une méthode nouvelle d'analyse phonospectroscopique utilisée dans la phoniatrie clinique*, Proc. XVI Intern. Congress on Logopedics and Phoniatrics, Interlaken 1974, Abstract in: Folia Phoniatrica, **26**, 3, 227 (1974).

[33] W. TŁUCHOWSKI, J. KACPROWSKI, W. MIKIEL, A. NIEDŹWIECKI, A. KOMOROWSKA, *Clinical phonospectroscopy — a preliminary report*, Otolaryngologia Polska, **29**, 3, 251-259 (1975) (in Polish, abstract in English).

[34] W. TŁUCHOWSKI, W. MIKIEL, R. GUBRYNOWICZ, W. KOMOROWSKA, *Acoustical examination of glottal movements in recurrent laryngeal palsy*, Proc. 4th Congress of the Union of European Phoniatricians, Wrocław 1975.

[35] W. TŁUCHOWSKI, W. MIKIEL, B. MANIECKA-ALEKSANDROWICZ, A. SZEWCZYK, *Phonospectroscopic investigations of physiological phonation activity of the larynx in pre-school children*, Proc. VI Days of Children Otolaryngology, Łódź 1977, Otolaryngologia Polska, **31**, Supplement, 150-151 (1977) (in Polish, abstract in English).

[36] H. WAKITA, G. FANT, *Toward a better model of the vocal tract*, STL-QPSR, 1, 9-29 (1978).

Received on May 4, 1979

ARCHIVES OF ACOUSTICS
4, 4, 305-316 (1979)

INVESTIGATIONS ON A POSSIBLE SUBSTITUTION OF RESONANT WOOD IN PLATES OF MUSICAL INSTRUMENTS BY SYNTHETIC MATERIALS*

D. HOLZ

Institut für Musikinstrumentenbau (DDR — 9657 Zwota)

Since resonant plates in stringed musical instruments are made from coniferous woods, particularly from spruce, with maximum quality requirements, investigations were carried out in order to test the use of other materials for this purpose. These were aluminium plates with two types of visco-elastic layer, and laminates of glass fibre reinforced epoxy and unsaturated polyester resin, with reinforcements of several types, but preferably unidirectional fibres. The conclusions resulting from the measured data of sound velocity and damping in the audible frequency range only encourage further research upon laminates of glass fibre reinforced plastics.

1. Introduction

As is well known, customary musical instruments with strings need radiating or resonant plates, e.g. the soundboard in a piano or the top plate in a violin or guitar. In some previous papers it was demonstrated [2, 3] that the acoustic efficiency of radiating plates depends on their bending stiffness, conditions of radiation, velocity and resistance of bending waves, mass per unit area, and damping.

These correlated magnitudes are referred to material qualities such as the modulus of elasticity E, the density ϱ, and the damping factor η', and to the dimensions of the plate, particularly the thickness. The value η' is defined by

$$\eta' = \frac{\Lambda}{\pi} = \frac{\Delta f}{f_R},$$

where Λ is the logarithmic damping decrement, f_R — the eigenfrequency in Hz, and Δf — the half power width.

* The first version of this paper was presented at the 22nd Open Seminar on Acoustics in Świeradów Zdrój, Poland, September 1975.

For optimally resonant wood a high E, a ϱ as low as possible, and a damping intermediate between those of metals and plastics, are demanded.

Such qualities agree with the rule that spruce, and perhaps a few other coniferous woods marked by specific parameters, are not only the best but possibly the sole materials for normal radiating plates. This is a due to the anisotropy of spruce and of woods in general, where the above-mentioned qualities are realized only along the grain (i.e. the fibre direction or beam axis), whereas perpendicular to the grain E is significantly smaller and η' is higher than the corresponding values for several other materials, including a number of plastics.

Frequently in the literature a high ratio for E/ϱ^3 called the acoustic constant or musical constant, is demanded, although some wood types as Balsa (Ochroma lagopus) or parasolier (Musanga smitthii), which have a very small density and thus a high "acoustic constant", have never been used or accepted as resonant wood. It was stressed in our previous work that the value of this ratio, claimed by HÖRIG [4] as "Strahlungsdämpfung" $\vartheta_s = 5 \cdot 10^{-3} \sqrt{E/\varrho^3}$ with omitted dimensions, is often overestimated, and that E/ϱ (or its square root, the sound velocity in bars) is particularly important for characterizing resonant wood. Thus interest should be taken in using other woods with a high E/ϱ and a lower E/ϱ^3. However, the decreasing supply of high-grade resonant wood in the world will, in the future, not correspond to its demand for the increasing production of musical instruments. Thus we have been involved in a search for other materials, in order to prepare a possible substitute for resonant wood in musical instruments in industrial production. There was no idea of using new materials in instruments manufactured by craftsmen.

2. Survey of possible substitutes

In looking for suitable substituting materials Figs. 1 and 2 may be considered useful. In Fig. 1 the relation between ϱ and E is shown for some groups of materials. Two straight lines have been drawn in this diagram: the line for all data of the important sound velocity $c_D = 5000\,\mathrm{m/s}$ and that for a high resonance ratio $Q_R = \sqrt{E/\varrho^3}$ of 10 $\mathrm{m^5/Ns^3}$ (we proposed this definition instead of "acoustic constant", which is only a quotient with omitted dimensions). Obviously such a high resonance ratio is valid only for a few woods; it is indeed even exceeded by few wood types such as those mentioned above but no other material can attain it.

A sound velocity of about 5000 m/s is given for several metals, such as iron, iridium, magnesium, and aluminium, and also for glass, porcelain, and, of course, for a number of woods. None of these materials, with the exception of wood, meets the condition of intermediate damping (Fig. 2). From this diagram it is evident that no individual, homogeneous material is suitable

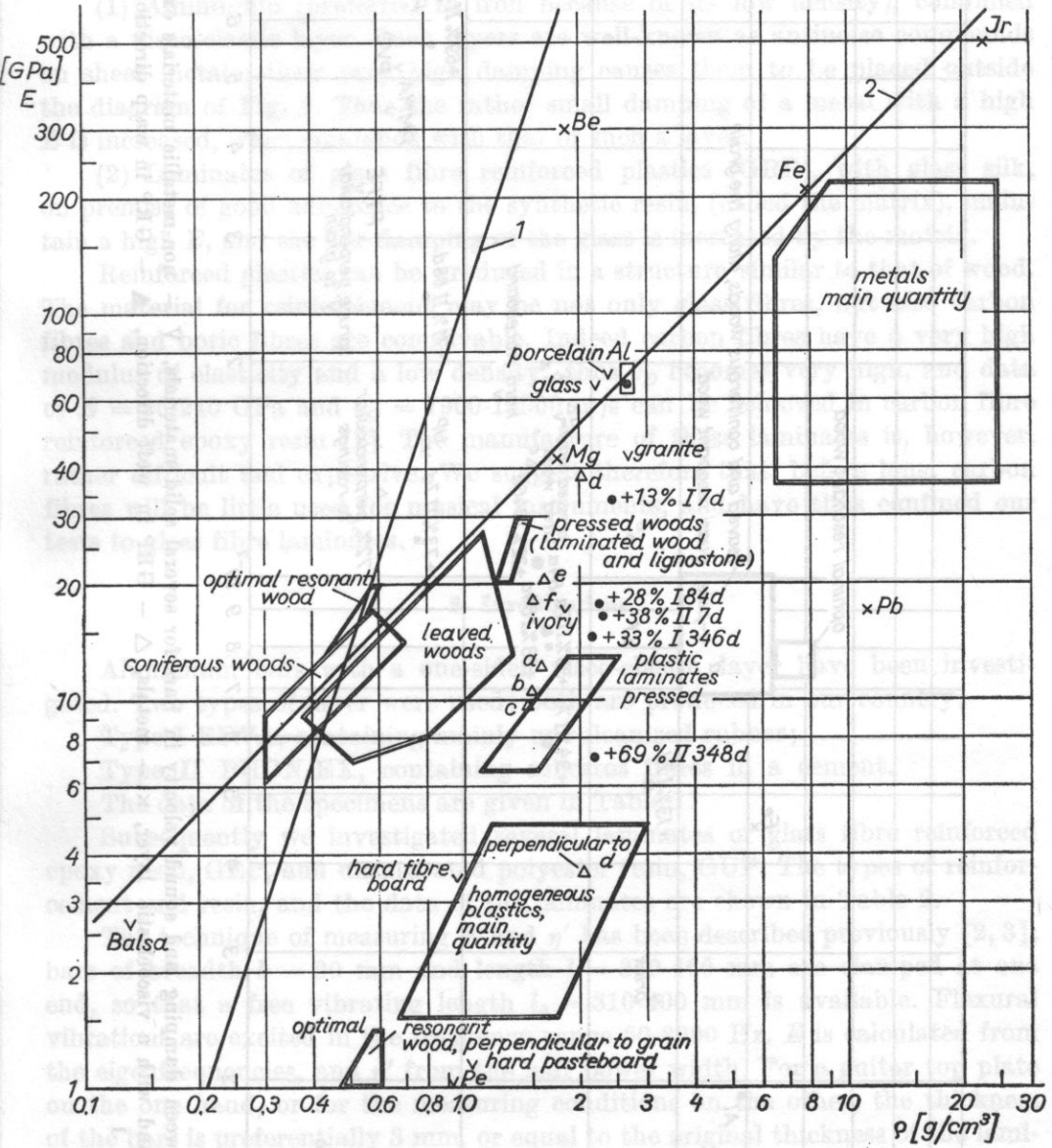

Fig. 1. Relation between density and modulus of elasticity for several solid metarials, V — non-metalic materials except GRP, • — aluminium only and with a visco-elastic layer, according to Table 1, x-metals, △ — glass fibre reinforced plastics (GRP), according to Table II; 1 — $Q_R = \sqrt{E/\varrho^3} = 10\ m^5/Ns^3$, 2 — $c_D = 5\,000$ m/s; glass fibre proportion and direction: (*a*) 55.7 % weft, (*b*) 29.4 % indifferent, (*c*) 45.4 % weft, (*d*) 72.0 %, rovings, (*e*) 55.7 % warp preferred, (*f*) 45.4 % warp preferred

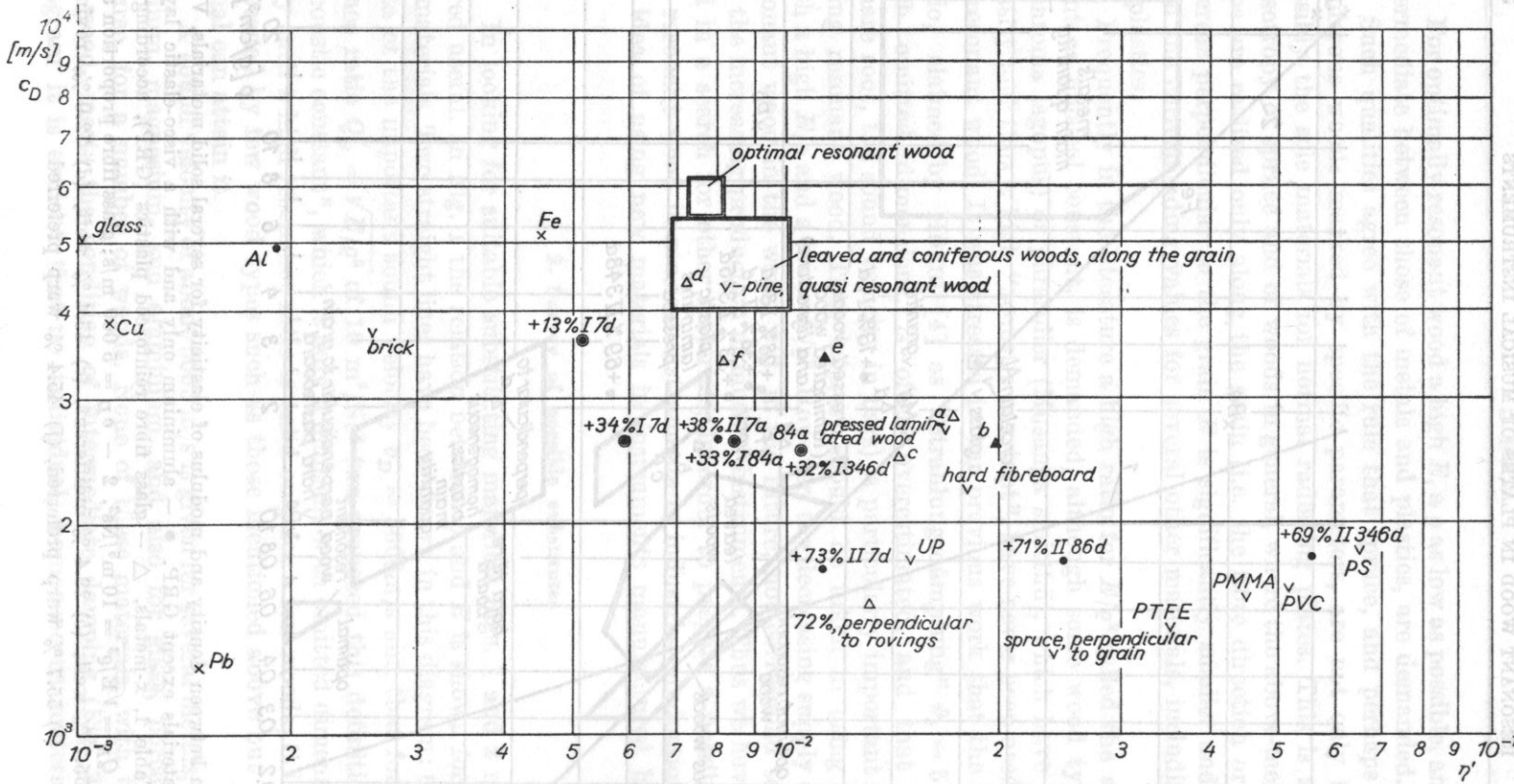

Fig. 2. Relation between damping and sound velocity in bars for several solid materials, V — non-metallic materials except GRP, ⊙. — aluminium only and with a viscoelastic layer, × — metals, △ — GRP in weft direction, ▲ — GRP in warp direction or preferred, a-f according to Fig. 1

for the substitution of resonant wood, but it appears possible to find a combination of two different materials. Two composite materials may be principally considered:

(1) Aluminium (preferred to iron because of its low density), combined with a visco-elastic layer. Such layers are well-known as antinoise compounds on sheet metals; their very high damping causes them to be placed outside the diagram of Fig. 2. Thus the rather small damping of a metal with a high E is increased, when combined with that of such a layer.

(2) Laminates of glass fibre reinforced plastics (GRP), with glass silk, on premise of good adherence to the synthetic resin, (called the matrix), maintain a high E, and the low damping of the glass is increased by the matrix.

Reinforced plastics can be produced in a structure similar to that of wood. The material for reinforcement may be not only glass fibres, but also carbon fibres and boric fibres are conceivable. Indeed carbon fibres have a very high modulus of elasticity and a low density, thus c_D becomes very high, and data of $E = 96\text{-}240$ GPa and $c_D = 7900\text{-}12500$ m/s can be achieved in carbon fibre reinforced epoxy resin [1]. The manufacture of these laminates is, however, rather difficult and expensive. We suggest therefore that, before long, carbon fibres will be little used for musical instruments, and have thus confined our tests to glass fibre laminates.

3. Investigations

Aluminium bars with a one-sided visco-elastic layer have been investigated. Two types of layer were used; both are produced in our country:

Type I EIWA, containing mainly unvulcanized rubber;

Type II PHON-EX, containing asbestos fibres in a cement.

The data of the specimens are given in Table 1.

Subsequently we investigated several laminates of glass fibre reinforced epoxy resin, GEP, and unsaturated polyester resin, GUP. The types of reinforcement and resin, and the data of the laminates are shown in Table 2.

The technique of measuring E and η' has been described previously [2, 3]; bars of breadth $b = 20$ mm and length $l = 350\text{-}460$ mm are clamped at one end, so that a free vibrating length $l_0 = 310\text{-}400$ mm is available. Flexural vibrations are excited in the frequency range 60-8000 Hz. E is calculated from the eigenfrequencies, and η' from the half power width. For a guitar top plate on the one hand, or for the measuring conditions on the other, the thickness of the bars is preferentially 3 mm, or equal to the original thickness of the laminate.

In view of the anisotropy of the laminates the bars were sawn in both warp and weft directions, i.e. in the direction of the rovings and perpendicular to it, respectively. The direction of the higher E is called the preferred or main direction. Results from the 2nd until the 24th eigenfrequency were obtained.

Table I. Aluminium bars with a layer of visco-elastic material for increase of damping

Material	Layer mass [%]	Specimen thickness [%]	Aging after coating d	Sound velocity [m/s]
aluminium only	0	3.0 mm = 100	—	4950
coated by EIWA (I)	13	125	7	3630
	34	165	7	2510
	33	163	84	2440
	32	162	346	2550
	28	155	7	2730
	28	153	84	2800
coated by Phon-Ex (II)	38	159	7	2640
	73	213	7	1740
	71	210	86	1770
	69	208	348	1790

Table II. Structure of investigated GRP-plates and GRP-bars

Designation	Resin type	Reinforcement material (E-glass), type	Glass mass [%]	Efficiency in warp (main) direction [%]
GRP – UP (GUP)	polyester	thin orthotropic* glass silk tissues, outwards; rude roving tissues, preferred in warp direction, inwards	55.7	85.5
GRP – EP (GEP)	epoxy	thin orthotropic glass silk tissues, outwards; rude roving tissues, preferred in warp direction, inwards	45.4	84.7
GUP	polyester	chopped strand mat, quasi isotropic	29.4	50
GUP	polyester	rovings only, unidirectional	72.0	100

* Orthotropic tissue, i.e. quadratic tissue quantities warp strings as much as weft strings.

Up to 2500 Hz not only flexural vibrations, but also some peaks of torsional vibrations and of quasilogitudinal waves were registered. From Fig. 3 it is

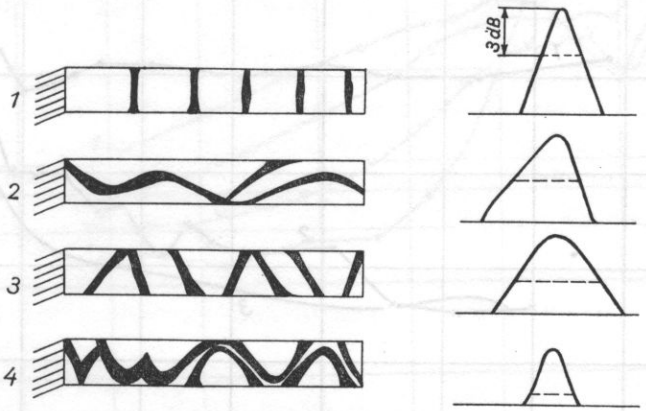

Fig. 3. Illustration of some different vibration nodes, by Lycopodium spores, and of their resonance curves (sole bending wave) : 1 $- f_R = 384$ Hz, 2 $- f_R = 480$ Hz, 3 $- f_R = 630$ Hz, 4 $- f_R = 2100$ Hz

obvious that the vibration nodes of such frequencies can be shown using Lycopodium spores. Symmetrical curves are attained by flexural waves, see $f_R = 384$ Hz.

4. Results

In all investigations the damping depends on the frequency (in the audible frequency range). As expected, the damping of aluminium with a visco-elastic layer increases, as the layer thickness increases. Due to the very low E of the layer compound itself, the E of the composite material decreases, as the layer thickness increases, and the sound velocity also diminishes. These results are seen in Figs. 1 and 2.

In principle a damping can be attained which closely approximates that of wood in any frequency range. This can be achieved by optimizing the layer thickness according to the type and properties of the layer compound. The dependence of damping upon frequency, Fig. 4, is nevertheless different from that of resonant wood. This fact is not as remarkable as the influence of aging upon damping. From Fig. 4 it is evident that η' varies over a period of time of nearly one year, not only as a result of drying but also because of aging of the visco-elastic material. It is probable that the age effects will last for at least two years.

In Fig. 5 the dependence of damping for GRP laminates is compared with that for resonant spruce along the grain. As is evident from Fig. 5a, rein-

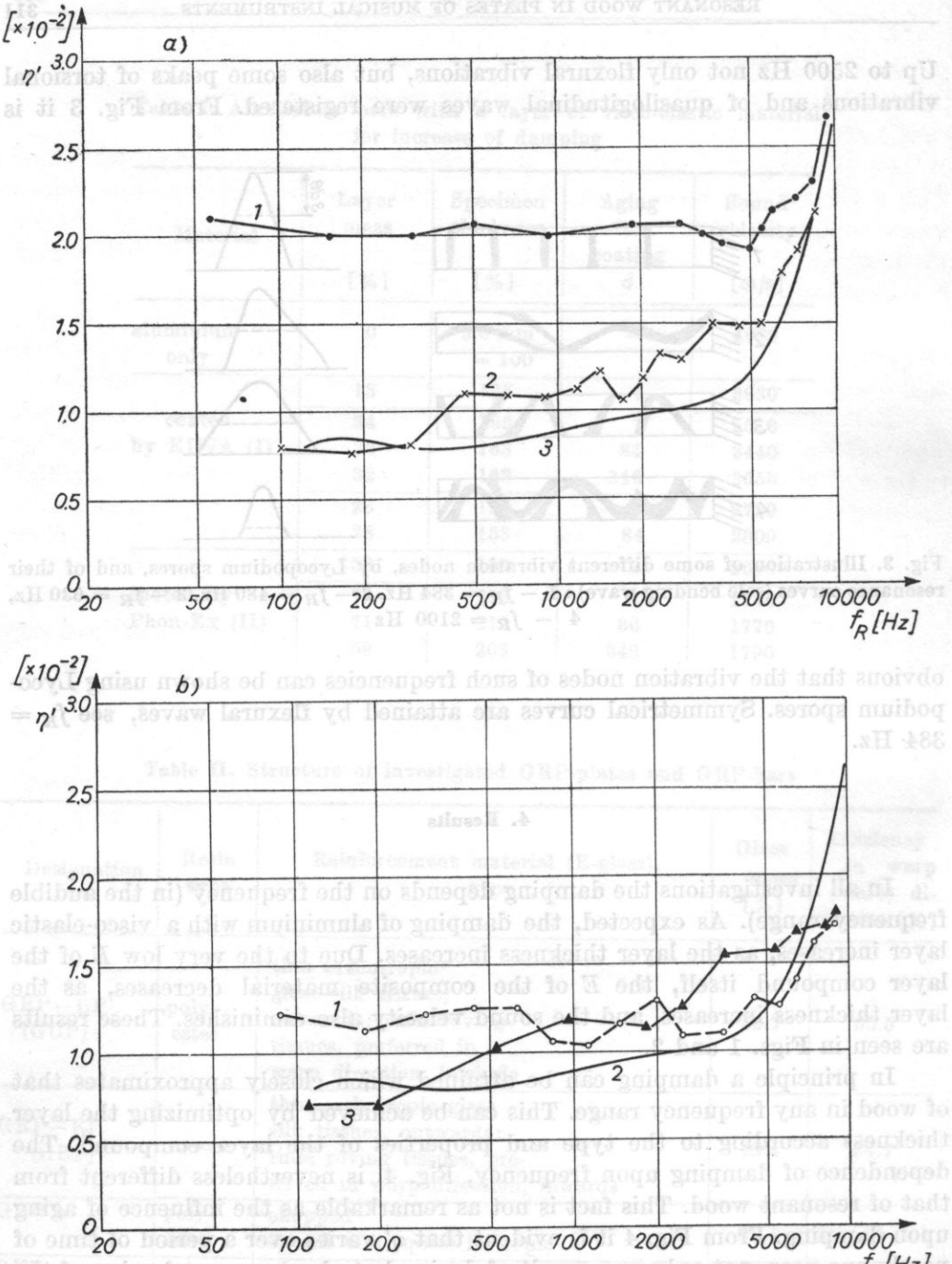

Fig. 4. Dependence of damping on frequency for glass fibre reinforced plastics: (a) epoxy resin (GEP), 1 – GUP, mat, glass 29,4 %, 2 – GUP in warp direction, tissue, glass mass 45.4 %, 3 – resonant spruce along the grain, (b) with PHON-EX (II), 1 – GUP, in warp direction, tissue, glass mass 55.7 %, 2 – resonant spruce along the grain, 3 – GUP in rovings direction, rovings only, glass mass 72 %.

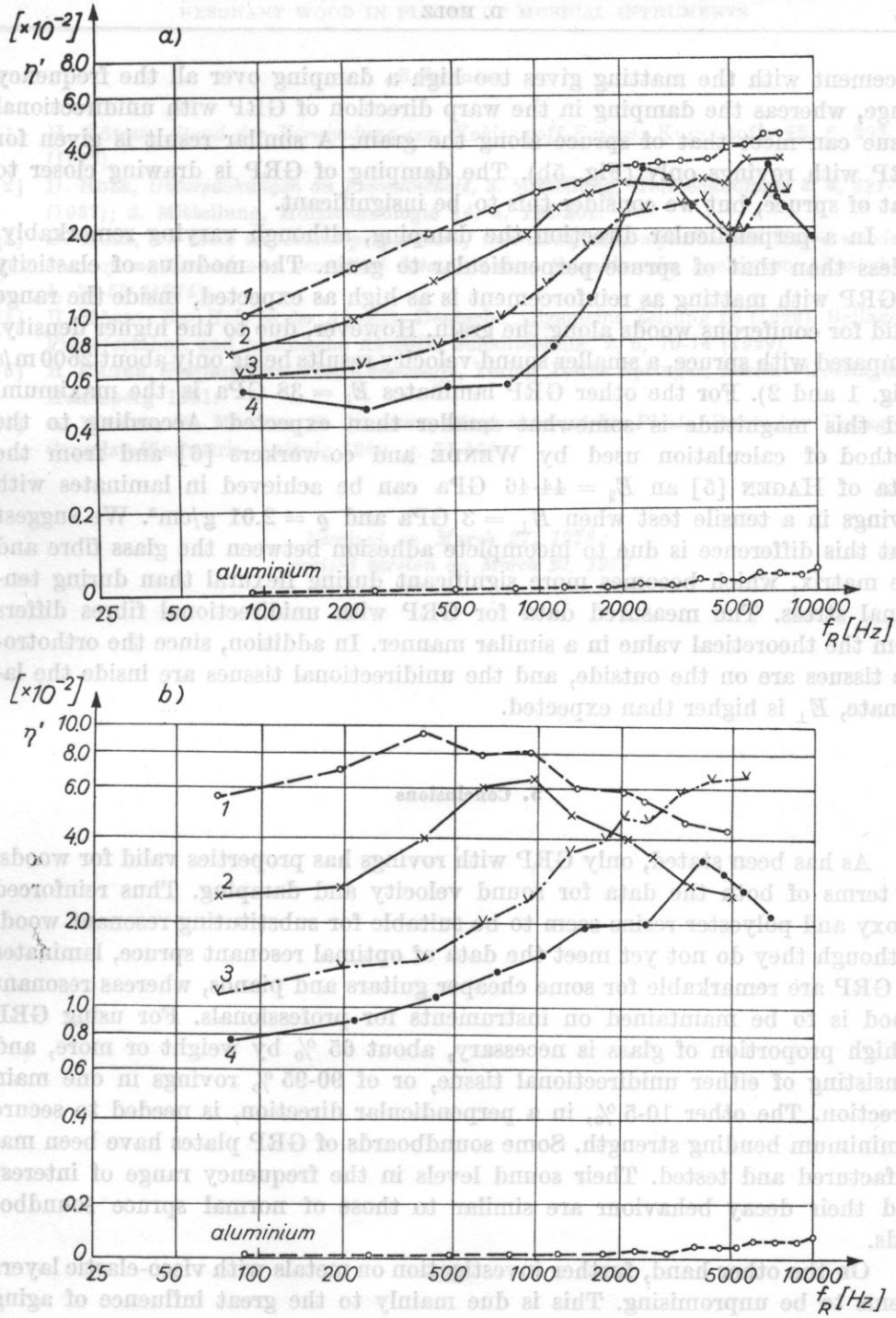

Fig. 5. Dependence of damping on frequency for aluminium only and with a visco-elastic layer, before and after natural aging at room temperature: (a) with EIWA (I) 1 – +31 %/346 d, 2 – +31 %/84 d, 3 – +31 %/7 d, 4 – +13 %/7d; (b) unsaturated polyester resin (GUP), 1 – +31 %/346 d, 2 – +71 %/86 d, 3 – +73 %/7d, 4 – 38 %/7d

forcement with the matting gives too high a damping over all the frequency range, whereas the damping in the warp direction of GRP with unidirectional tissue can meet that of spruce along the grain. A similar result is given for GRP with rovings only (Fig. 5b). The damping of GRP is drawing closer to that of spruce, but we consider this to be insignificant.

In a perpendicular direction the damping, although varying remarkably, is less than that of spruce perpendicular to grain. The modulus of elasticity of GRP with matting as reinforcement is as high as expected, inside the range valid for coniferous woods along the grain. However, due to the higher density, compared with spruce, a smaller sound velocity results being only about 2600 m/s (Fig. 1 and 2). For the other GRP laminates $E_{\parallel} = 38$ GPa is the maximum, and this magnitude is somewhat smaller than expected. According to the method of calculation used by WENDE and co-workers [6] and from the data of HAGEN [5] an $E_{\parallel} = 44\text{-}46$ GPa can be achieved in laminates with rovings in a tensile test when $E_{\perp} = 3$ GPa and $\varrho = 2.01$ g/cm³. We suggest that this difference is due to incomplete adhesion between the glass fibre and the matrix, which becomes more significant during flexural than during tensional stress. The measured data for GRP with unidirectional fibres differs from the theoretical value in a similar manner. In addition, since the orthotropic tissues are on the outside, and the unidirectional tissues are inside the laminate, $E_{\perp}$ is higher than expected.

5. Conclusions

As has been stated, only GRP with rovings has properties valid for woods, in terms of both the data for sound velocity and damping. Thus reinforced epoxy and polyester resins seem to be suitable for substituting resonant wood. Although they do not yet meet the data of optimal resonant spruce, laminates of GRP are remarkable for some cheaper guitars and pianos, whereas resonant wood is to be maintained on instruments for professionals. For using GRP a high proportion of glass is necessary, about 65 % by weight or more, and consisting of either unidirectional tissue, or of 90-95 % rovings in one main direction. The other 10-5 %, in a perpendicular direction, is needed to secure a minimum bending strength. Some soundboards of GRP plates have been manufactured and tested. Their sound levels in the frequency range of interest and their decay behaviour are similar to those of normal spruce soundboards.

On the other hand, further investigation on metals with visco-elastic layers seems to be unpromising. This is due mainly to the great influence of aging upon the damping, which cannot be predetermined, and also by the very small modulus of elasticity of the layer material. This behaviour does not meet the demands of quality for any radiating plate.

References

[1] H. Böder, *Stand der Verwendung von Kohlenstoff-Fasern*, Kunststoffe **62**, 5, 293-296 (1972).

[2] D. Holz, *Untersuchungen an Resonanzholz*, 3. Mitteilung, Holztechnologie **8**, 4, 221-224 (1967); 5. Mitteilung, Holztechnologie **14**, 4, 195-202.

[3] D. Holz, *On some important properties of non-modified coniferous and leaved woods in view of mechanical and acoustical data in Piano Soundboards*, Archiwum Akustyki **9**, 1, 37-57 (1974).

[4] H. Hörig, *Das Holz in der Akustik*, Deutsche Allgemeine Zeitung 25 (1929), Beilage – Pianofortebau und technische Akustik, Schalltechnik, **2**, 5, 70-74 (1929).

[5] H. Hagen, *Glasfaserverstärkte Kunststoffe*, Verlag Julius Springer, Berlin – Göttingen – Heidelberg 1961.

[6] A. Wende, W. Moebes, H. Marten, *Glasfaserverstärkte Plaste*, Deutscher Verlag für Grundstoffindustrie, Leipzig 1969, p. 71-180.

Received on March 27, 1978;
revised version on March 30, 1979

ARCHIVES OF ACOUSTICS
4, 4, 317-330 (1979)

CORRELATION AND PULSE TECHNIQUES FOR IDENTIFICATION OF THE PATHS OF DIFFRACTED AND PENETRATING WAVES THROUGH BARRIERS

STEFAN CZARNECKI

Institute of Fundamental Technological Research, Polish Academy of Sciences (00-049 Warszawa)

ZBIGNIEW ENGEL, ANNA MIELNICKA

Institute of Mechanics and Vibroacoustics, Mining and Metallurgy Academy (30-059 Kraków)

This paper presents a theoretical analysis and the results of measurements aimed at distinguishing in the total energy transmitted by the barrier, the energy of a wave penetrating the barrier due to its limited insulation and the energy of a wave diffracted at the edge of the barrier.

Correlation and pulse techniques have been used in the investigation, to compare the resolution of the two methods for chosen kinds of acoustic signals, i.e. for band noise in the correlation method and for a pulse produced by a spark source in the pulse method. The calculated uncertainty products were the basis for the comparison of resolution agreement between the two methods.

1. Introduction

Problems in the identification of both sound sources and the paths of acoustic waves propagation are among the basic considerations of vibroacoustics. They are primarily significant for vibroacoustic diagnostics and for noise control, since a quantitative determination of acoustic energy at an observation point of an acoustic field permits to find the dominant source or the dominant propagation path.

The basic phenomenon used for identification of the paths of acoustic energy transmission through the barrier is the difference in the arrival times of acoustic waves propagating by different paths from the source to the observation point behind the barrier.

The primary difficulty in the identification of the paths of sound transmission is the limited resolution of a method, which permits the signals reaching the

observation point to be distinguished. Sufficiently large differences in paths are necessary to distinguish distinctly the acoustic signals of a specific kind.

Of different identification methods two methods are noteworthy which are opposed to each other from the point of view of time character of acoustic signals: the correlation method using quasistationary signals and the pulse method using the momentary signals.

The resolution of the two methods is limited by the Heisenberg uncertainty principle which combines the necessary time and frequency intervals of the signal investigated, in order to maintain the adequate analytical conditions. However, due to the differences in the signals, the measuring apparatus, and the purposes of the investigation, the usefulness of the two methods may differ [5].

The aim of this paper is to use both methods for the identification of transmission paths of acoustic waves through the barrier. For the sake of simplification only two kinds of paths were considered: the path of a wave penetrating through the barrier and the path of a diffracted wave on its upper edge.

In addition to the theoretical aspects, the present problem has also a practical significance. The methods that are analyzed in the paper permit a suitable material to be selected in the barrier designing to predict the proper insulation properties of the barrier due to its dimensions. The practical significance of the methods presented in this paper is particularly conspicuous in the measurements carried out under the real conditions.

2. Previous investigations on the use of correlation and pulse techniques for the testing of the barrier

The correlation technique has for many years been used in acoustical research. It was very early used in GOFF's investigations [9] of the effectiveness of IL (Insertion Loss) of boards, which he determined from the measured cross-correlation function between the signal supplying the loudspeaker and the signal of acoustic pressure measured behind the board. Goff obtained experimental results which were close to the calculated results according to the mass law, with a very high precision of 1 dB.

WHITE [13] analyzed the possible uses of the correlation technique as the method for identification of systems involving many paths of acoustic wave propagation. His papers were not concerned with acoustic barriers; however, the approach which he developed can be partly used for the analysis of a wave transmitted through the barrier and of a diffracted wave.

Using a method combining the correlation technique and Fourier analysis, SCHOMER [11] obtained the best results in the identification of diffracted and penetrating waves. He investigated the cross-correlation function of sound pressures measured at given points in front of and behind the barrier. Subsequently, he measured the Fourier transform for relevant sections of the curves

of the cross-correlation function, thus determining the transmittance of the ith path of acoustic wave transmission through the barrier.

Schomer's results were in agreement with the calculated results only over the frequency range where the source had a flat frequency response, with a deviation of $\pm$ 3 dB.

The pulse methods were used to investigate partition walls, with only penetrating waves being analyzed [1, 3, 4]. However, there have been no papers concerning the investigation of waves diffracted on the barrier edge by the pulse methods.

3. Analysis of properties of the barrier

Of many possible propagation paths of acoustic waves trough the barrier, the present paper discusses only two: the path of a wave diffracted on the upper barrier edge and the path of a wave penetrating the barrier due to its limited insulation.

The following quantities have been assumed for the description of acoustic properties of the barrier:

— the barrier effectiveness for a penetrating wave

$$\mathrm{IL}_p = 10 \log \frac{p_0^2}{p_p^2} \quad [\mathrm{dB}], \tag{1}$$

— the barrier effectiveness for a diffracted wave

$$\mathrm{IL}_d = 10 \log \frac{p_0^2}{p_d^2} \quad [\mathrm{dB}], \tag{2}$$

where individual values of mean-squared acoustic pressures are: p_0^2 — for a direct wave, p_p^2 — for a wave penetrating the barrier, p_d^2 — for a wave diffracted on the upper barrier edge.

A coefficient of weighting of transmitted energies can be introduced as a quantity which would quantitatively define the proportions of energies carried by a diffracted and a penetrating wave to the observation point:

$$\gamma = \frac{p_d^2}{p_p^2}. \tag{3}$$

It is convenient to represent this coefficient on the logarithmic scale as the weighting level of transmitted energies, which will be called the weighting level:

$$L_{pd} = 10 \log \gamma = \mathrm{IL}_d - \mathrm{IL}_p \quad [\mathrm{dB}]. \tag{4}$$

The barrier effectiveness for the penetrating wave can be expressed by the law of mass

$$\mathrm{IL}_p = 10 \log \left(\frac{\pi f m}{\varrho c} \right)^2 \quad [\mathrm{dB}], \tag{5}$$

where f is the acoustic wave frequency, m — mass per unit barrier area, ϱ — density of the medium, c — sound speed of acoustic wave.

The barrier effectiveness for a diffracted wave after the MEAKAWA's formula can be expressed as

$$\mathrm{IL}_d = 10 \log 20\, NK = 10 \log 0.12\, f\delta K \,[\mathrm{dB}] \quad \text{for } N > 1, \tag{6}$$

where N is a Fresnel number, $N = 2\delta/\lambda$, δ — difference in paths of a diffracted wave and a direct wave, λ — acoustic wave length.

The coefficient K represents the kind of sound source and its directivity. For the source of spherical wave the coefficient K is given [8] by the formula

$$K = \frac{x_d^2}{x_0^2}, \tag{7}$$

where x_d^2 and x_0^2 are the sound paths of the diffrected and direct wave, respectively. Based on relations (5) and (6), the expression for the weighting level L_U can take the form

$$L_{pd} = 10 \log \frac{f m^2}{\varrho^2 c^2 \delta K} + 9.3 \quad [\mathrm{dB}]. \tag{8}$$

4. Methods for identification of sound transmission paths through the barrier

The basic phenomenon used for the identification of sound transmission paths through the barrier is the difference in arrival times of acoustic waves propagating by various paths from the source and the observation point behind the barrier. Fuzziness of transmitted signals due to the measurement technique or to nonuniform propagation paths is the main difficulty here.

Principal limitations between the resolving powers of the signal in the time and frequency domains result from the Heisenberg uncertainty principle. Filtering the signal with a narrow transmission band Δf causes the signal to be fuzzy in time, making the separation of signals and their quantitative analysis difficult.

(a) **The correlation method.** White noise or filtered noise with a width Δf is the source of acoustic signal in the correlation method. The correlation method which

can determine the barrier effectiveness for respective paths can be used to find the transmission paths of acoustic waves through the barrier – in the present case, the paths of a diffracted wave and a wave penetrating the barrier.

As in Fig. 1, the cross-correlation function is determined from two signals delayed with respect to each other: the reference signal $X_1(t)$ received from the point M_1 and the measuring signal $X_2(t)$ from the point M_2. The signal $M_2(t)$ is delayed with respect to the signal $X_1(t)$ by a time dependent on the passage time of acoustic wave from the point M_1 to the point M_2. These delays are: for a direct wave τ_0, for a penetrating wave τ_p, and for a diffracted wave τ_d. Assuming a small barrier thickness relative to a distance r_0 between the points M_1 and M_2, it can be accepted that $\tau_0 = \tau_p$. Thus the barrier effectiveness can be determined after GOFF's [9] relation: for the path of a diffracted wave

$$\mathrm{IL}_u = 10 \log \frac{R_{xy0}(\tau_0)}{R_{xyd}(\tau_d)} \quad [\mathrm{dB}], \tag{9}$$

and for the path a penetrating wave

$$\mathrm{IL}_t = 10 \log \frac{R_{xy0}(\tau_0)}{R_{xyp}(\tau_0)} \quad [\mathrm{dB}], \tag{10}$$

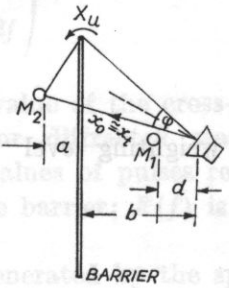

Fig. 1. A schematic diagram of the measuring system

where $R_{xy0}(\tau_0)$ is the maximum of the cross-correlation function for a direct wave without the barrier with a delay τ_0, $R_{xyd}(\tau_d)$ – the maximum of the cross--correlation function for a wave diffracted on the upper barrier edge with a delay τ_d, and $R_{xyp}(\tau_0)$ is the maximum of the cross-correlation function for a wave penetrating the barrier with a delay $\tau_p = \tau_0$.

As a parameter defining the ratio of energies transmitted through the barrier by the two paths, the weighting coefficient (expression (3)) will be

$$\gamma = \frac{R_{xyd}(\tau_d)}{R_{xyp}(\tau_0)} \quad [\mathrm{dB}]. \tag{11}$$

Thus the weighting level expressed by term (4) will take the form

$$L_{pd} = 10 \log R_{xyd}(\tau_d) - 10 \log R_{xyp}(\tau_0) = \mathrm{IL}_d - \mathrm{IL}_p \quad [\mathrm{dB}]. \tag{12}$$

(b) **The pulse method.** If the input signal is an acoustic pulse of a sufficiently short duration relative to the difference $\tau_d - \tau_p$, the signal received will consist of two separate pulses corresponding to the pulse penetrating the barrier and the pulse diffracted on the barrier edge.

From the pulse response function $p(t)$ the sought quantities which describe

the acoustic properties of the barrier can be determined: the barrier effectiveness for a penetrating wave

$$\mathrm{IL}'_p = 10 \log \frac{\int_0^{T_1} p_0^2(t)\,dt}{\int_{T_1}^{T_2} p_d^2(t)\,dt}, \tag{13}$$

the barrier effectiveness for a diffracted wave

$$\mathrm{IL}'_d = 10 \log \frac{\int_0^{T_1} p_0^2(t)\,dt}{\int_0^{T_1} p_p^2(t)\,dt}, \tag{14}$$

the weighting level

$$L'_{pd} = 10 \log \frac{\int_{T_1}^{T_2} p_d^2(t)\,dt}{\int_0^{T_1} p_p^2(t)\,dt}, \tag{15}$$

where the time interval 0-T corresponds to the interval in which the penetrating wave reaches the observer, the time interval $T_1 - T_2$ corresponds to the interval in which the diffracted wave reaches the observer.

The methods mentioned above for the determination of the weighting level between the diffracted and penetrating waves assume a high sharpness of signals obtained by both correlation and pulse methods. In practice these signals are fuzzy due to the limited resolution of the aparatus in the domains of time and frequency, resulting from the Heisenberg principle,

$$U = \Delta f \Delta t \leqslant A, \tag{16}$$

where Δt is the minimum difference between the passage times of acoustic wave by various paths from the source to the observer, permitting the successive signals to be distinguished, Δf is the minimum band width of the filter which gives correct analytical results for a given value of Δt, A is a constant dependent on the kind of signal. The expression $\Delta t \Delta f$ is called the uncertainty product [2]. Since the envelopes of the cross-correlation curves including maxima are not rectangular, the problem occurs how to establish suitable averaging criteria permitting the inambiguous determination of the values of Δt and Δf. Of many known criteria of signal width, the variance of squared amplitude modulus was used in the present investigation as the measure most convenient for the

oscillating signal which appears in the correlation method and to some degree also in the pulse method,

$$(\Delta t)^2 = \frac{\int_{-\infty}^{+\infty} t^2 |p(t)|^2 dt}{\int_{-\infty}^{+\infty} |p(t)|^2 dt} - \left(\frac{\int_{-\infty}^{+\infty} t |p(t)|^2 dt}{\int_{-\infty}^{+\infty} |p(t)|^2 dt} \right)^2 \tag{17}$$

and

$$(\Delta f)^2 = \frac{\int_{-\infty}^{+\infty} f^2 |F(f)|^2 df}{\int_{-\infty}^{+\infty} |F(f)|^2 df} - \left(\frac{\int_{-\infty}^{+\infty} f |F(f)|^2}{\int_{-\infty}^{+\infty} |F(f)|^2 df} \right)^2, \tag{18}$$

where $p(t)$ in the correlation method is the maximum value of the cross-correlation function corresponding to the penetrating or diffracted waves; in the pulse method — the corresponding maximum values of pulses representing the diffracted wave and the wave penetrating the barrier; $F(f)$ is the Fourier transform of the function $p(t)$.

In the paper, the uncertainty products for noise generated by the spark source U' were calculated from formulae (17) and (18). The values of the uncertainty products can be a basis for comparison of the resolution of the two methods, since a better resolution corresponds to a smaller value of the uncertainty product.

5. The experimental investigations

A pressed chipboard barrier with dimensions 4.1m × 1.8 m and 2 cm thick was used in the investigations. The experiment was carried out under the free field conditions, placing the barrier in an anechoic chamber in order to limit the waves reflected from the surfaces of the room, and also the waves transmitted from sources in adjacent rooms.

The barrier was suspended on a steel rope from the ceiling of the chamber in order to eliminate structure-borne sound carried by the base. The source-barrier-observer geometry was chosen so that at the observation point the energy of the wave diffracted on one edge of the barrier was considerably greater than the energies of waves diffracted on the other edges. The position of the barrier and the measuring points during the investigation is shown in Fig. 1. The investigations were carried out for three positions of the sound source with respect to the barrier (for different distances b).

In the correlation method a reference signal from a reference microphone placed at a distance $d = 10$ cm from the loudspeaker for all the positions investigated was used.

The delays τ_p of the penetrating wave and τ_d for the diffracted wave at the microphone M_2 related to the arrival times of the signal to the reference microphone M_1 were respectively

$$\tau_0 = \tau_p = \frac{x_{p-d}}{c}, \quad \tau_d = \frac{x_{d-d}}{c}, \tag{19}$$

where x_p and x_d are the path lengths of the penetrating and diffracted waves respectively. The delays τ_d, τ_p for correlation method and τ'_d, τ'_p for pulse method calculated for individual positions are shown in Table 1.

Table 1. Delays τ for chosen measuring geometries

Geometry No.	b [cm]	Correlation method			Pulse method		
		τ_p [ms]	τ_d [ms]	$\tau_d - \tau_p$ [ms]	τ'_p [ms]	τ'_d [ms]	$\tau'_d - \tau'_p$ [ms]
I	40	1.5	2.9	1.4	2.1	3.5	1.4
II	60	1.9	3.3	1.4	2.5	3.8	1.3
III	80	2.4	3.7	1.3	3.0	4.3	1.3

The cross-correlation function of sound pressures measured by the microphones M_1 and M_2 was determined using an LT 213 Histomat Intertechnique correlator. White noise filtered in 1/3 octave bands at centre frequencies of 4, 6.3, 8, 10, 12.5 and 16 kHz was used as the signal in the correlation method.

Pulses generated by the spark source filtered in the same bands as in the correlation method were used in the pulse method. The pulse response function of the system investigated was measured using a 7503 type Brüel and Kjaer pulse recorder.

Further calculations aimed at determination of the uncertainty products for the two measurement methods were performed using a digital computer ODRA 1325.

In order to decrease the error resulting from the directional characteristics of the source, the loudspeaker was placed at such an angle with respect to the horizontal surface that its axis coincided with the bisector of the angle between the rays of the direct wave and of the wave falling on the upper edge of the barrier (Fig. 1).

Two methods of estimating the quantities measured were used in the two measuting techniques:

1. Consideration of the maximum values of the functions $R_{xy}(\tau)$ and $|p(t)|^2$ in chosen intervals. This was called the *method of maximum values.*

2. Consideration of the values of the integral from the squared functions $R_{xy}(\tau)$ and $|p^2(t)|$ in the same intervals as in point (1). This was called the *method of averaged values.*

6. The experimental results

The results of measuring the barrier effectiveness for the penetrating wave (formula (10)) and for the diffracted wave (formula (11)) for the three barrier-source-observer geometries and the measurement results obtained using the correlation and pulse methods with the two estimation techniques are shown in Tables 2 and 3. The results of calculations and measurements of the weighting level for the diffracted and penetrated waves for the data in Tables 2 and 3 are shown in Table 4 and Figs. 2 and 3. The values of the uncertainty product obtained by the correlation and pulse methods for individual source-barrier-observer geometries and also the mean values of U_{av} are shown in Table 5.

7. Conclusions

The following conclusions may be drawn from the investigations performed:

1. Determination of the weighting level between the diffracted and penetrating waves in a given frequency band is possible with a single measurement using the correlation or pulse methods.

2. Despite of the common limitation of the correlation and pulse methods due to the uncertainty principle, the two methods show different resolution due to the difference in the acoustic signals used.

3. Quantitative comparison of the resolution of the present methods can be made by calculation of the uncertainty numbers with the assumed signal widths in the domains of time and frequency. A better resolution of the method corresponds to a smaller uncertainty number. In the experiment the pulse technique showed a better resolution.

4. From the separate analysis of the diffracted and the penetrating waves it was found that the resolution of the two methods is better for the diffracted wave than for the penetrating wave. This proves the effect of additional factors such as dispersion or complex impedance which may occur when the wave penetrating the barrier.

5. Investigation of the barrier using the present methods showed a good agreement between the calculated and measured results. The mean absolute deviation of the measured and calculated results did not exceed 1 dB for all the quantities measured. In both methods the choice of the estimate showed a large effect on the investigation results. The method of averaged values showed a better agreement between the measured and calculated results.

6. The present method of identification of propagation paths of acoustic waves through the barrier can be expanded to include other propagation paths, e.g. those of reflected waves. When considering a greater number of paths,

Table 2. The barrier effectiveness for a wave penetrating the barrier

Middle frequency of 1/3 octave band	Geometry I					Geometry II					Geometry III				
	Correlat. method		Pulse method		Cal.	Correlat. method		Pulse method		Cal.	Correlat. method		Pulse method		Cal.
	IL_{pm}	IL_{pav}	IL'_{pm}	IL'_{pav}		IL_{pm}	IL_{pav}	IL'_{pm}	IL'_{pav}		IL_{pm}	IL_{pav}	IL'_{pm}	IL'_{pav}	
Hz	dB														
4 000	29.4	31.7	31.2	30.1	30.8	29.8	31.9	31.1	31.8	30.8	33.2	32.5	32.2	31.6	30.8
6 300	34.2	34.5	34.3	34.9	34.8	35.7	34.5	34.1	35.4	34.8	36.3	33.7	35.4	35.8	34.8
8 000	36.5	37.3	35.7	36.2	36.8	36.1	37.3	37.5	36.6	36.8	37.5	36.6	36.3	37.2	36.8
10 000	38.0	38.2	39.7	38.6	38.8	39.4	39.0	38.1	39.6	38.8	39.7	39.1	38.2	40.0	38.8
12 500	40.0	41.7	40.1	41.4	40.8	41.0	40.3	39.9	41.3	40.8	41.5	40.0	40.5	41.0	40.8
16 000	44.5	43.2	41.7	42.5	42.8	42.0	43.2	43.5	43.1	42.8	42.5	42.1	41.7	43.5	42.8

m – maximum value; av – average value

Table 3. The barrier effectiveness for a wave diffracted by the barrier

Middle frequency of 1/3 octave band	Geometry I					Geometry II					Geometry III				
	Correlat. method		Pulse method		Cal.	Correlat. method		Pulse method		Cal.	Correlat. method		Pulse method		Cal.
	IL_{dm}	IL_{dav}	IL'_{dm}	IL'_{dav}		IL_{dm}	IL_{dav}	IL'_{dm}	IL'_{dav}		IL_{dm}	IL_{dav}	IL'_{dm}	IL'_{dav}	
Hz	dB														
4 000	27.2	28.5	28.0	26.6	28.2	26.1	27.7	28.1	27.3	26.9	28.2	26.2	27.4	26.1	25.8
6 300	31.1	30.9	29.9	30.9	30.2	28.5	28.7	28.8	29.3	28.9	28.5	26.1	27.5	29.0	27.8
8 000	32.9	30.7	28.8	31.3	31.2	29.8	30.3	29.8	29.3	29.9	29.2	28.0	29.0	29.6	28.8
10 000	32.2	31.7	32.4	32.2	32.2	33.6	30.8	29.8	30.4	30.9	30.7	30.3	28.2	31.2	29.8
12 500	29.2	34.8	32.0	31.2	33.2	32.5	33.4	31.0	31.8	31.9	30.8	31.1	30.2	31.2	30.2
16 000	34.5	33.5	32.3	35.6	34.2	33.4	32.3	33.5	32.3	32.9	31.4	33.0	31.8	32.4	31.8

m – maximum value; av – average value

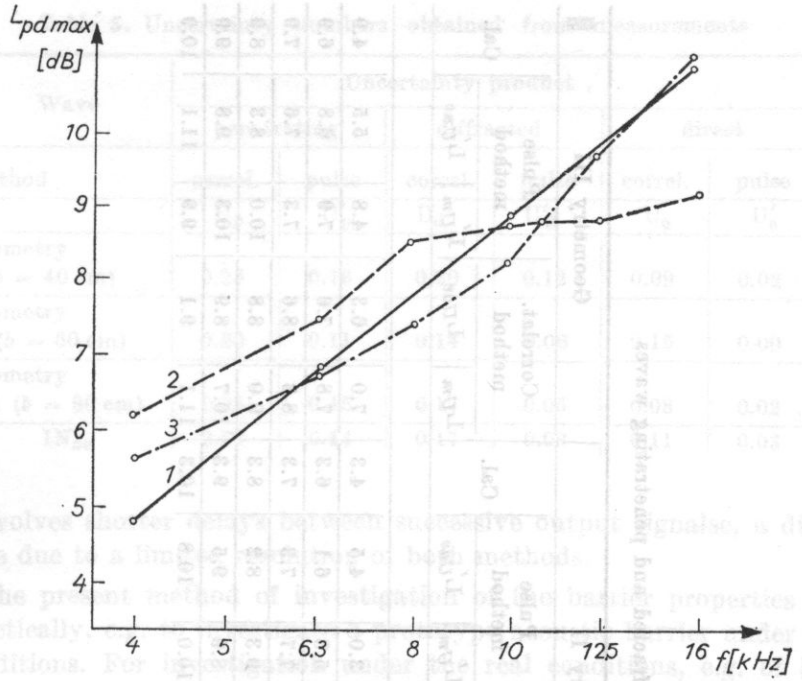

Fig. 2. The weighting level ($a = 10$ cm, $b = 60$ cm), with consideration of the maximum values
1 – calculation results, 2 – results of measurements by correlation method, 3 – results of measurements by pulse method

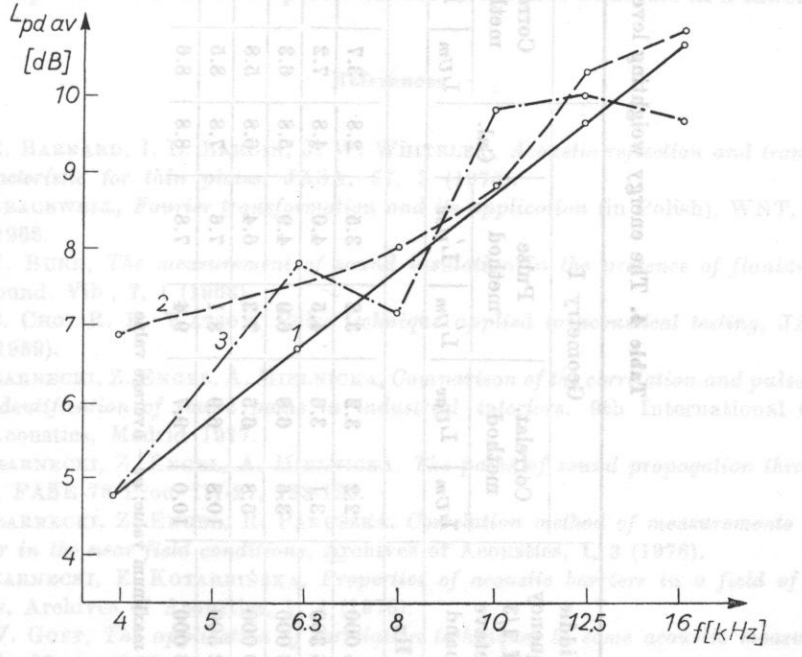

Fig. 3. The weighting level ($a = 10$ cm, $b = 60$ cm), with consideration of averaged values
1 – calculation results, 2 – results of measurements by correlation method, 3 – results of measurements by pulse method.

Table 4. The energy weighting level for diffracted and penetrating waves

Middle frequency of 1/3 octave band	Geometry I					Geometry II					Geometry III				
	Correlat. method		Pulse method		Cal.	Correlat. method		Pulse method		Cal.	Correlat. method		Pulse method		Cal.
	L_{Um}	L_{Uav}	L'_{Um}	L'_{Uav}		L_{Um}	L_{Uav}	L'_{Um}	L'_{Uav}		L_{Um}	L_{Uav}	L'_{Um}	L'_{Uav}	
Hz	dB														
4 000	2.2	3.2	3.2	3.5	2.8	3.7	4.2	3.0	4.5	4.3	7.0	6.3	4.8	5.5	4.9
6 300	3.1	3.6	4.5	4.0	4.8	7.2	5.8	5.3	6.1	6.3	7.8	7.6	7.9	6.8	6.9
8 000	3.6	6.6	6.9	4.9	5.8	6.3	7.0	7.7	7.3	7.3	8.3	8.6	7.3	7.6	7.9
10 000	5.8	6.5	7.3	6.4	6.8	5.8	8.2	9.3	8.2	8.3	9.0	8.8	10.0	8.3	8.9
12 500	10.8	6.9	8.1	7.6	7.8	8.5	9.8	8.9	9.5	9.3	10.7	8.9	10.3	9.8	9.9
16 000	10.0	9.7	9.4	7.8	8.8	8.6	10.9	10.0	10.8	10.3	11.1	9.1	9.9	11.1	10.9

m – maximum value; *av* – average value

Table 5. Uncertainty numbers obtained from measurements

Wave	Uncertainty product					
	penetrating		diffracted		direct	
method	correl.	pulse	correl.	pulse	correl.	pulse
	U_p	U'_p	U_d	U'_d	U_0	U'_0
geometry I (b = 40 cm)	0.25	0.16	0.20	0.12	0.09	0.02
geometry II (b = 60 cm)	0.20	0.11	0.14	0.08	0.15	0.00
geometry III (b = 80 cm)	0.28	0.15	0.17	0.05	0.08	0.02
IN_{av}	0.24	0.14	0.17	0.08	0.11	0.03

which involves shorter delays between successive output signalse, a difficulty may arise due to a limited resolution of both methods.

7. The present method of investigation of the barrier properties can be used practically, e.g. to investigate a prototype acoustic barrier under laboratory conditions. For investigation under the real conditions, e.g. of barriers in industrial interriors with real noise sources only the correlation method seems valid. It involves the recording of the input and output signals on the magnetic tape recorder and the performance of further analysis in a laboratory.

References

[1] G. R. Barnard, I. L. Bardin, J. W. Whiteley, *Acoustic reflection and transmission characteristic for thin plates*, JASA, **57**, 3 (1975).

[2] R. Bracewell, *Fourier transformation and its application* (in Polish), WNT, Warszawa 1968.

[3] A. N. Burd, *The measurement of sound insulation in the presence of flanking paths*, J. Sound. Vib., **7**, 1 (1968).

[4] A. C. Cho, R. B. Watson, *Pulse technique applied to acoustical testing*, JASA, **31**, 10 (1959).

[5] S. Czarnecki, Z. Engel, A. Mielnicka, *Comparison of the correlation and pulse methods for identification of sound paths in industrial interiors*, 9th International Congress on Acoustics, Madrid 1977.

[6] S. Czarnecki, Z. Engel, A. Mielnicka, *The paths of sound propagation through barriers*, FASE-78 Proc. III-27, 123-126.

[7] S. Czarnecki, Z. Engel, R. Panuszka, *Correlation method of measurements of sound power in the near field conditions*, Archives of Acoustics, **1**, 3 (1976).

[8] S. Czarnecki, E. Kotarbińska, *Properties of acoustic barriers in a field of reflected waves*, Archives of Acoustics, **1**, 4 (1976).

[9] K. W. Goff, *The application of correlation techniques to some acoustic measurements*, JASA, **27**, 2 (1955).

[10] K. Mańczak, *Methods of identification of multidimensional controlled systems* (in Polish), WNT, Warszawa 1971.

[11] P. D. SCHOMER, *Measurement of sound transmission loss by combining correlation and Fourier techniques*, JASA, **51**, 4 (1972).

[12] V. V. SOLODNIKOV, *Statistical dynamics of automatic control linear systems* (in Polish), WNT, Warszawa 1964.

[13] P. H. WHITE, *Cross-correlation in structural systems, dispersion and nondispersion waves*, JASA, **45**, 2 (1969).

Received on April 6, 1979

ARCHIVES OF ACOUSTICS
4, 4, 331-346 (1979)

AN ACOUSTICAL AID FOR THE BLIND

ZBIGNIEW MARCIN WÓJCIK

Space Research Centre of Polish Academy of Sciences
(00-716 Warszawa, ul. Bartycka 18)

Aids for the blind, used so far, which transform images to touch stimuli, are not faultless. The low resolution of mechanical operative systems and the elasticity of skin reduce practical usefulness of these aids. The aid which equivalently transforms optical images to acoustic signals is free from the faults mentioned above.

It follows from physiological investigations of the brain that the right hemisphere of one born blind can take over a parallel analysis of optical images transferred by acoustic signals. A blind person who lost sight later in his life can recognize optical images transmitted by sound by way of an analysis mainly carried out by the left hemisphere of the brain. The left hemisphere usually performs a serial data analysis.

The present paper discusses the transformation of optical images to corresponding equivalent acoustic signals, and also presents a design for the electronic system of an acoustical aid. This system should become a valuable device in research, and it may also be applied practically in future.

1. Introduction

It is obvious that information can be transferred to a blind person by acoustic signal. In order to enable a blind person to receive optical images by his hearing organ, a physical measurable carrier of visual information must be equivalently transformed to acoustical signals. After some training, a blind person will be able to translate these signals into optical images.

Black and white optical images that are invariable in time, e.g. black and white photographs, are usually represented in the Cartesian reference system composed of the *Oxy* plane of an opto-electrical converter screen (Fig. 1), and the light energy axis parallel to it. This threedimensional diagram represents a physical form of an optical image. The analysis of images that are variable in time requires successive, time discrete analyses of the threedimensional diagram. In the paper, however, we shall concentrate on the static images only.

2. The idea of transforming an optical image to an acoustic signal

The idea of an acoustical aid as presented in this paper is that of equivalent transformation of the physical form of a visual image to an acoustic signal. Since the spectrum of an acoustic signal analyzed by man is usually represented in a coordinate system of energy-frequency-time (Fig. 2) there are several possible variants of such transformation. It follows from Figs. 1 and 2 that both diagrams have a common axis, i.e. the axis of energy (or amplitude) of a signal. Thus no special converters are necessary for coding an optical image into an acoustic signal during transformation of these axes, with a possible exception of an electronic signal amplifier. The other two axes: Ox and Oy in the diagram of a visual image (Fig. 2) can be transformed in the following way:

$$tx : Ox \rightarrow \text{time}, \tag{1a}$$

$$ty : Oy \rightarrow \text{frequency} \tag{1b}$$

or, conversely,

$$tx : Ox \rightarrow \text{frequency}, \tag{2a}$$

$$ty : Oy \rightarrow \text{time}, \tag{2b}$$

where tx, ty are symbols for these transformations.

Relation (2a) represents an exact assignment of each tone of a frequency f_X to each screen element (Fig. 1) with its coordinate X on the Ox-axis of the screen. It follows from relation (2b) that the illumination energy of any screen element (Fig. 1) with its coordinate Y on the Oy-axis of the screen reference diagram is transformed into sound only within a specific time interval $t(Y)$ which is equivalent to the coordinate Y. The reference time for each interval $t(Y)$ is defined by a certain specific sound produced in a time interval $t(0)$ before the process of transformation of an optical image begins. After generation of a reference sound at a time $t(0)$, successive lines of the screen, $Y = 1, 2, 3, \ldots, N$ are transformed to acoustic signals. Since fastest possible transformation is required we shall try to achieve as short a time interval $t(y)$ as possible. On the other hand, $t(Y)$ must not be too short on the account of masking phenomena due to the sounds received by hearing in the time intervals $t(Y-1)$ and $t(Y+1)$. The number of the tones $\{f_1, f_2, \ldots, f_X, \ldots, f_M\}$ discriminated by man is also limited, amounting to about 600 [13] for an average musical hearing. Problems in the resolution of an acoustical aid for the blind will be shown in section 5 of this paper.

It follows from (2a) and (2b) that a light object equal in size to an element (X, Y) of the screen that is against a light background is transformed to a tone f_X occurring in a time interval $t(Y)$ after generation of a reference sound at a time $t(0)$. Since hearing sensations in man are directly proportional to the

logarithm of energy of sounds being heard, and also the signal amplitude at the opto-electrical converter output is directly proportional to the illumination energy of the photosensitive half-tone screen mosaic, a subjective reception of the intensity of a tone f_X is directly proportional to the logarithm of lightness of an object.

The use of function (1) causes the following sensation of the position of the object:

— the location in the horizontal direction — as a time interval between the time signalled and the time of hearing a tone exceeding all other adjacent tones in energy;

— while the location in the vertical direction — as the pitch (frequency) of the tone.

The presence of several such objects in the image analyzed causes several different tones to occur at various time intervals. Differences of lightness of these objects result in sensation of equivalent intensities of these tones.

The dimensions of these objects are proportional to:

1. Using function (1):

(a) dimensions in the direction of the Ox-axis (horizontal) — durations of tones exceeding all other tones in energy,

(b) dimensions in the direction of the Oy-axis (vertical) — the number of tones heard;

2. Using function (2), conversely:

(a) horizontal dimensions — the number of tones heard,

(b) vertical dimensions — durations of these tones.

Distances from objects to a blind person are measured by the position of the depth of focus in the optical system through which the images investigated are projected onto the opto-electrical converter. The depth of focus can be manually adjusted by a blind person. If there are objects in the depth of focus as determined by a blind person (sensed through touch), their presence is signalled by corresponding tones. If there are not, white noise due to a uniform unfocussed background and the internal noise of the converter can be heard. If the objects are at the limits of focus depth, the optical image is fuzzy and the sounds received are close to white noise. Tones heard are indistinct. Even a slight change in the position of focus depth causes a considerable change in tone articulation (the articulation of a tone f_X is here the ratio of the energy of this tone to the energy of tones f_{X-1} and f_{X+1}).

The presence of sounds corresponding to optical images investigated that are close to white noise, is the acoustical criterion for focus depth adjustment. The focus depth is selected so that the energy ratios of tones $f_X, f_{X+1}, \cdots, f_{X+n}$, to tones $f_{X-m}, f_{X-m+1}, \cdots, f_{X-1}$ and also tones $f_{X+n+1}, f_{X+n+2}, \cdots, f_{X+n+k}$ is maximum or minimum.

3. The overal structure of the acoustical aid for the blind

Currently used optoelectrical converters use sequential scanning, i.e. the following elements of the screen S are analyzed successively in time:

$$\begin{aligned} S = {} & p(1,1), p(2,1), \ldots, p(X,1), \ldots, p(M,1), \\ & p(1,2), p(2,2), \ldots, p(X,2), \ldots, p(M,2), \\ & \ldots\ldots\ldots\ldots\ldots\ldots\ldots\ldots\ldots\ldots \\ & p(1,Y), p(2,Y), \ldots, p(X,Y), \ldots, p(M,Y), \\ & \ldots\ldots\ldots\ldots\ldots\ldots\ldots\ldots\ldots\ldots \\ & p(1,N), p(2,N), \ldots, p(X,N), \ldots, p(M,N), \end{aligned} \tag{3}$$

where $p(X, Y)$ are coordinates with indexes X, Y on the optoelectrical converter screen (Fig. 1).

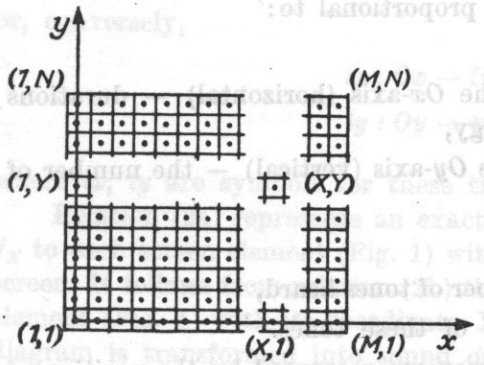

Fig. 1. Ideal half-tone screen of the opto-electrical converter (i.e. photosensitive mosaic net on to which a visual image is projected)

The equivalent transformations (1) or (2) of an optical image to acoustic signals are retained if whole screen lines are simultaneously being transformed. The time sequence of these transformations is

$$\{1, 2, \ldots, Y, \ldots, N\} = L, \tag{4}$$

i.e. from the bottom to the top of the screen (Fig. 1). The set L of the screen lines is therefore orderly. The optical image transformation from expressions (2a) and (2b) requires:

(a) memorizing of the values of elements $1,2, \ldots, X, \ldots, M$ of the Y line of the screen, $Y \in L$;

(b) transformation of the Y line to a signal F,

$$F = \sum_{X=1}^{M} f(X, Y) = \sum_{X=1}^{M} v(X, Y) k(X), \tag{5}$$

where $k(X)$ is a constant level of the generator output signal at a frequency equivalent to the X column of the screen; $v(X, Y)$ is the value of the opto-electrical converter output signal, corresponding to a screen element with coordinates $p(X, Y)$ and modulating a signal $k(X)$ $f(X, Y)$ is the amplitude of a signal over the range of acoustic frequencies that is equivalent to the X column of screen elements, modulated by the signal $v(X, Y)$; M is the number

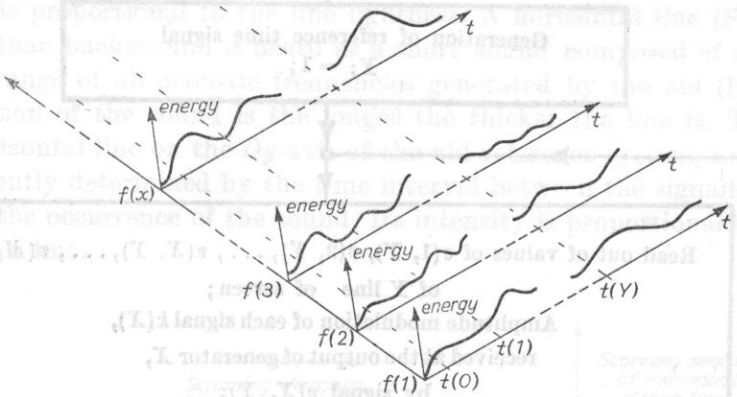

Fig. 2. Physical information carrier of sound signal; the real time spectrum of sound

of signals at various acoustic frequencies generated by the aid; M is at the same time the number of the optoelectrical screen elements in one line of the screen;

(c) elimination from memory of the values of elements of the Y line of the screen and storing in memory of the values of a successive screen line, $Y+1$.

This process repeats cyclically as in point (b) until all values of the screen elements have been read. The functional diagram for the acoustical aid is shown in Fig. 3.

It should be noted that it is possible to build an aid which can successively transform individual screen elements (formula (3)) to individual tones. This aid however would be M times slower, compared to the aid whose functional diagram is shown in Fig. 3. The aid operating according to the algorithm in Fig. 3, using relation (2) to transform static optical images, will be discussed later in the paper. Transformation of selected elements of graphic images such as straight lines of different finite thicknesses, arcs and curves of these lines and so forth will be also considered.

After beginning of each cycle of transforming an arbitrary optical image to an acoustical signal, a sound signal is generated which means that the image to sound transformation is beginning. After a single transformation of all the screen lines to an acoustical signal, another reference sound signal is generated, and the aid working cycle is repeated (Fig. 3). Thus the beginning of each scanning of the whole screen is signalled. The beginnings of scanning of successive lines are not signalled.

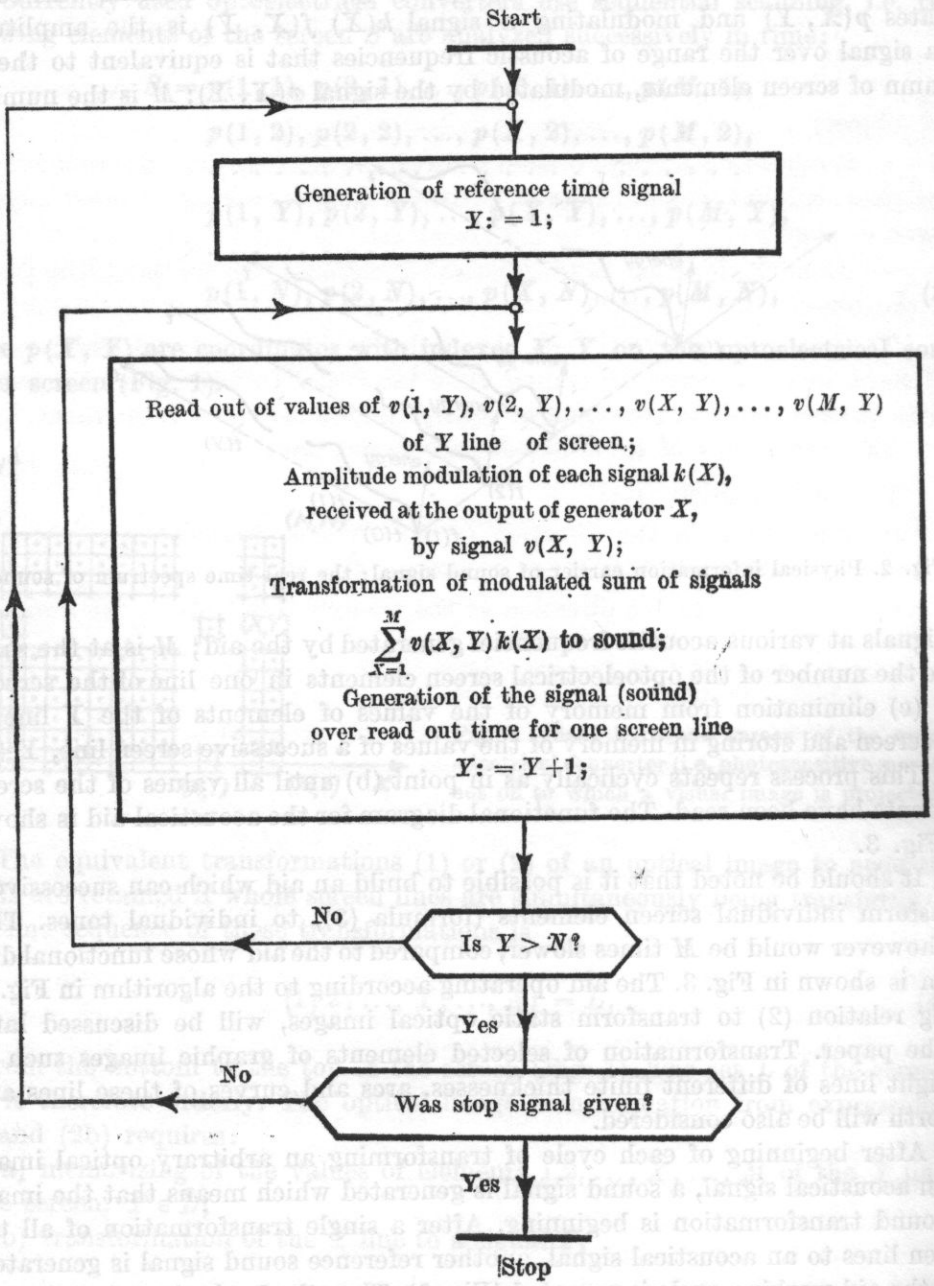

Fig. 3. Functional diagram of the acoustical aid conform to relation (2), with memorizing of the values of elements of whole screen lines

A vertical straight line (Fig. 4a) that is lighter than background is transformed by the aid to a sound composed of a certain number of tones. The thinner the line is, the fewer tones occur. The tones occur throughout the observation of the line, i.e. without changing in any of the time intervals separated by reference signals.

The frequencies of these tones equivalently determine the position of the line on the Ox-axis of the screen reference system, i.e. horizontally. The sound intensity is proportional to the line lightness. A horizontal line (Fig. 4b) that is lighter than background is heard as a short sound composed of all the tones over the range of all acoustic frequencies generated by the aid (formula (5)). The duration of the sound is the longer the thicker the line is. The position of the horizontal line on the Oy-axis of the aid reference system, i.e. vertically, is equivalently determined by the time interval between the signalled reference time and the occurrence of the sound. Its intensity is proportional to the lightness of the line.

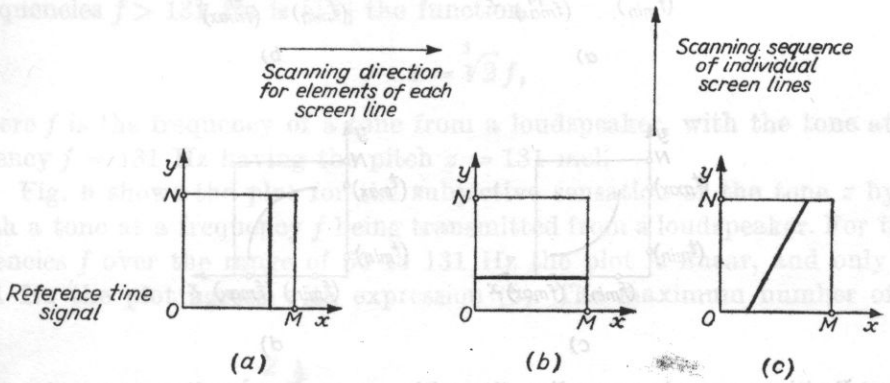

Fig. 4. Positions of straight line on the screen of the opto-electrical converter: (*a*) vertical line, (*b*) horizontal line, (*c*) line inclined at an acute angle relative to the Ox-axis of the screen reference system

The same straight line inclined at an acute angle with respect to the Ox-axis of the screen reference system (Fig. 4c) is heard as a sound composed of a number of tones. The number of these tones decreases with decreasing thickness of the line. Its loudness is proportional to the lightness of the image. The frequencies of the tones of the sound increase linearly in time. The increase rate is the greater the more inclined the line is (the more acute its angle is relative to the Ox-axis of the screen reference system — Fig. 4c). The duration of the sound perception also decreases with decreasing angle a. A line that is lighter than background, inclined at an acute angle with respect to the Ox-axis of the screen is heard in an analogous manner — however the frequencies of the audible sound tones increase in time.

When the curve of the concave line being transformed by the aid, which is lighter than background, is positive (due to the sign of the first derivative — Fig. 5a), the frequencies of sound tones heard increase in time less and less than linearly. When the curve of the convex line being analyzed by the aid, which is lighter than background, is positive (Fig. 5b), the frequencies of sound tones heard by a blind person increase faster and faster (faster than linearly). The loudness of these tones is proportional to the lightness of images. The number of these tones is proportional to the thickness of images in the directions of the *Ox*-axis of the screen. The positions of successively analyzed in time fragments of light images in the observation field of the aid — in the directions

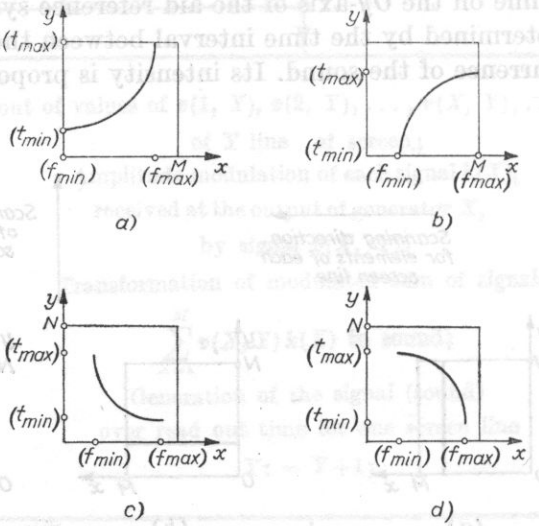

Fig. 5. (*a*) Positive curve of concave line, (*b*) positive curve of convex line, (*c*) negative curve of concave line, (*d*) negative curve of convex line

of the *Oy*-axis of the screen, i.e. vertically — correspond to the time intervals between the reference times and the appearance times of these tones, which are equivalent to the images. Durations of these tones are proportional to the widths of objects in the direction of the *Oy*-axis of the screen. The minimum (t_{min}) and the maximum (t_{max}) time intervals between the reference and appearance times correspond to the extreme positions of the images analyzed by the aid, in the direction of the *Oy*-axis of the screen (Fig. 5). Current frequencies of the tones heard equivalently define the positions of light images being analyzed by the aid in the directions of *Ox*-axis of the screen. The widths of images in the horizontal direction, i.e. in the direction of the *Ox*-axis of the screen, correspond to the number of the sound tones. The lowest (f_{min}) and the highest (f_{max}) frequencies of these tones equivalently define the extreme positions of these sound tones of the investigated light object in the direction of the *Ox*-

axis of the screen. The loudness of these tones equivalently corresponds to the lightness of individual fragments of images. If the curve of the concave lighter-than-background line analyzed by the aid is negative (due to the sign of the first derivative of the line — Fig. 5 c), the sound can be heard that is composed of tones whose frequencies decrease more and more slowly (more slowly than linearly). Analogously, the negative curve of the convex lighter-than-background line results in tones whose frequencies decrease faster than linearly i.e. faster and faster (Fig. 5d).

It is now hard to predict how useful the aid will be for recognition of complex geometrical figures such as letters. It is certain however to be useful in recognizing large, simple objects such as greens, streets and pavements, walls of houses, light windows, and strong lamps.

4. Possibilities of perceiving optical images by hearing

The subjective sensation of the pitch z of a tone by hearing, for acoustic frequencies $f > 131$ Hz is [13] the function

$$z = \sqrt[3]{2}\, f, \tag{6}$$

where f is the frequency of a tone from a loudspeaker, with the tone at a frequency $f = 131$ Hz having the pitch $z = 131$ mel.

Fig. 6 shows the plot for the subjective sensation of the tone z by man, with a tone at a frequency f being transmitted from a loudspeaker. For the frequencies f over the range of 50 to 131 Hz the plot is linear, and only above 131 Hz the plot agrees with expression (6). The maximum number of tones

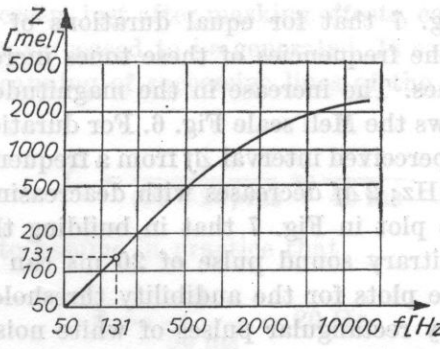

Fig. 6. The plot for subjective sensation of the pith z of a tone by hearing in relation with the frequency f of the tone [13]

heard, neglecting the masking effects, does not exceed $z = 2400$ mel. An average man perceives more than 600 different tones [13]. In building an acoustical aid 600 generators can be used, each generating a tone with the pitch z, according

to the diagram in Fig. 6. An arbitrary, successive pitch z must be higher than the preceding by at least $\sqrt[3]{2}$, beginning with $f = 131$ Hz.

For the acoustic frequencies $f < 131$ Hz, however,

$$z = f. \tag{7}$$

Due to the system assumed for the transformation of optical images, the pitch z must have a discrete behaviour:

$$f_X := z. \tag{8}$$

Fig. 7 shows three plots for the maximum frequency variation Δf perceived by man for tones at frequencies $f = 0.25$ kHz, 1 kHz, 4 kHz as a function of duration t_i of these tones. The tones were produced by sine pulses. Each of the three plots was made for the tones f separately.

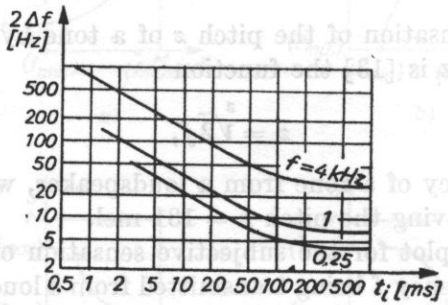

Fig. 7. The minimum perceptible variation Δf of a tone at a frequency f in relation with durations t_i of these tones [13]

It follows from Fig. 7 that for equal durations of arbitrary tones, the variation perceived in the frequencies of these tones increases with increasing frequencies of these tones. The increase in the magnitude of variation in frequencies perceived follows the Meli scale Fig. 6. For durations t_i of sound pulses longer than 200 ms, the perceived interval Δf from a frequency f does not change. $2\Delta f = 7$ Hz for $f = 1$ kHz; $2\Delta f$ decreases with deacreasing f.

It follows from the plot in Fig. 7 that in building the aid for the blind, a duration t_i of an arbitrary sound pulse of 20 ms can be assumed.

Fig. 8b shows three plots for the audibility threshold L(dB) of Gaussian sound pulses, masked by rectangular pulses of white noise, in relation to the interval Δt between the white noise and Gaussian pulses. These pulses are schematically shown in Fig. 8a; S is the intensity of white noise rectangular pulses, L is the intensity of Gaussian pulses. At an intensity L of Gaussian pulses, after a time Δt from the end of the rectangular masking white noise pulses at an intensity S, the Gaussian pulses begin to be perceived by human hearing. From the plot, the sound which corresponds to any Y line on the opto-

electrical converter screen is masked by the sound corresponding to the preceding line, $Y - 1$, of the screen. Assuming in building the aid a mean level of the sound generated by the acoustical device, equal to 80 dB $= S = L$ (Fig. 8), we obtain the interval between two arbitrary sound pulses equal at least to 20 ms. This interval is necessary to minimize the effect of masking on the hearing of an arbitary, successive sound pulse. Masking effects analogous to those in Fig. 8b occur when white noise is transmitted from a loudspeaker in pulses after the generation of Gaussian sound pulses (conversely to Fig. 8a).

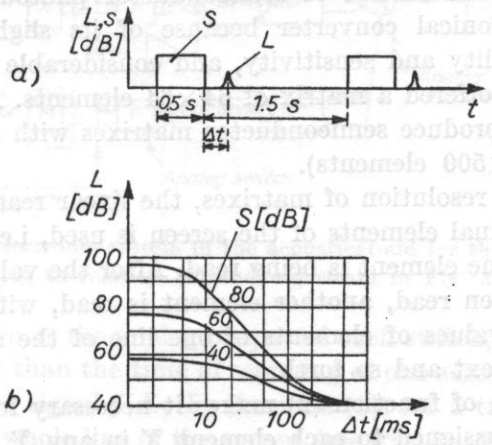

Fig. 8. (*a*) Graphic interpretation of Gaussian sound pulses L from a loudspeaker after a time Δt from the generation of rectangular white noise pulses S, (*b*) Audibility threshold L (dB) of Gaussian sound pulses, each of 30 ms duration, masked by white noise with an intensity S(dB) before generation of masked pulses [13]

In practice, it is possible to generate an arbitrary sound pulse, corresponding to any Y line of the screen, just after masking effects, corresponding to the $Y - 1$ line of the screen have ceased to be generated. It can thus be assumed that the frequency f_w of scanning of successive lines of the optoelectrical converter screen is

$$f_w = \frac{1}{(20+20)\text{ ms}} = \frac{1}{40\text{ ms}}.$$

It seems better to assume in practice that

$$f_w = \frac{1}{50\text{ ms}} = 20\text{ Hz}.$$

It is thus possible to convey to the blind about 20 lines of the screen within one second by sound pulses. It seems also difficult to increase the dimensions of the screen in the direction of the Oy-axis, i.e. vertically, since the optical image conveyed as a series of sound pulses in real time would be fuzzy; the movements of a blind person cause the image observed to move on the screen

of the converter. It is however possible to read the image quickly, e.g. within 1/50th of a second, transfer it to the memory of the aid and equivalently transform the memorised image into a series of sound pulses, according to the algorithm shown in Fig. 3.

5. Construction of the electronic system of the acoustical aid

The self-contained matrix of semiconductor photodetectors is the most suitable opto-electronical converter because of its slight dimensions, small weight, high reliability and sensitivity, and considerable resolution. E.g. IPL has for some years offered a matrix of 64×64 elements. American companies, e.g. RCA, already produce semiconductor matrixes with a resolution of a TV camera (over 500×500 elements).

Due to a large resolution of matrixes, the linear readout of the values of signals from individual elements of the screen is used, i.e. at each moment at most the value of one element is being read. After the value of the signal from one element has been read, another element is read, with the readout being orderly: since the values of elements of one line of the screen are read, first then those of the next and so forth.

The application of function (2) makes it necessary for each tone $f(X, Y)$ to be equivalently assigned to each element X in any Y line, to each column X of the screen elements (see formula (5)). The intensity of this tone is proportional to the value $v(X, Y)$ of the signal received at the output of the element $p(X, Y)$,

$$\forall\big(p(X, Y) \in S\big)\big(f(X, Y) = k(X) \cdot v(X, Y)\big), \tag{9}$$

where $k(X)$ is the amplitude of a signal at a frequency corresponding to the X column of the screen, $\forall$ is a general quantifier ($\forall\big(p(X, Y) \in S\big)$ means: for each element $p(X, Y)$ in the set S (see formula (3))).

As follows from the above, a hearing aid consists of an M set of generators (M is the number of elements in one screen line — Fig. 1), with every X-generator giving an output signal $f(X, Y)$ (formula (5)), proportional to the value of lightness of the X, Y element of the screen, i.e. to $v(X, Y)$. Since the matrix is scanned linearly, a distributor must be built permitting the introduction of the value $v(X, Y)$ to a relevant generator X. The distributor can be made of a looped, series-parallel shift register with M bits, M outputs and 1 input, coupled with the time base of the readout of the photodetector matrix [8] where at the beginning of the read out of the whole matrix only one 1 is introduced. Fig. 9 shows a block diagram of the aid. The start of the matrix readout determines the signalled reference time for the perception of the position of objects vertically. As follows from Fig. 9, this moment is defined by the tone f_X. One-channel analog switches, e.g. C-MOS type [5] are designated

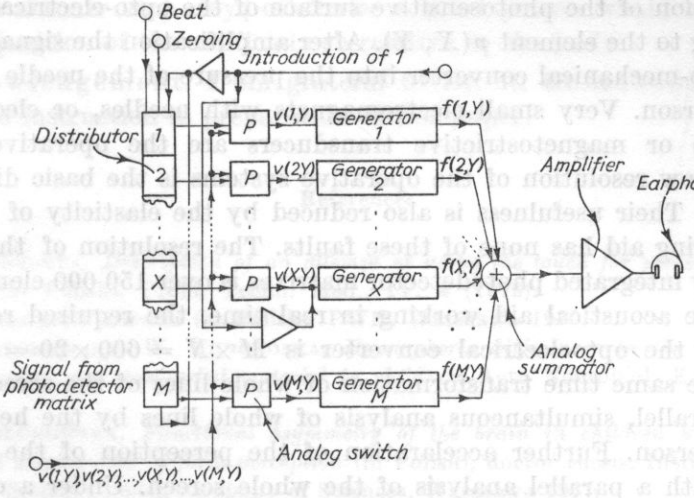

Fig. 9. A design of the electronic system in the acoustical aid for the blind, working according to relation (2) and algorithm in Fig. 3

as P in Figure 9. Since at the analog output of each switch, the switching pulse lasts M times shorter than the time of scanning of one screen line, each generator X should generate signal $f(X, Y)$ (formula (5)) for a time τ_M equal to the readout time for one whole line of the screen (see Fig. 3). The time τ_M cannot be shorter than 40 ms (see point 4). Thus the time of storing the output signal of any analog switch can be close to the scanning time τ_M for one screen line.

Each generator X consists of a unit generating a signal $k(X)$ with a constant amplitude, which is modulated by a signal $v(X, Y)$ received at the output of the photodetector column X.

The values of constant signals $k(1), k(2), \ldots, k(X), \ldots, k(M)$, affecting the values of modulated signals $f(1, Y), f(2, Y), \ldots, f(X, Y), \ldots, f(M, Y)$ (formulae (5) and (9)), can have a distribution over the range of acoustic frequencies close to the speech spectrum.

6. Conclusions

Blind people still have no suitable device which would enable them to receive visual sensations in a satisfactory manner. The designers of visual aids are at present working towards enabling the blind to receive visual stimuli by touch receptors in the skin. The designs of suitable miniature opto-mechanical converters are becoming better due to the development of technology. These converters operate in the following way [7]: the optical image is projected on to the screen of the opto-electrical converter which is a table of $M \times N$ elements. The electrical signal received at the output of an arbitrary element $p(X, Y)$ of the screen is proportional to the illumination (or to its logarithm)

of a tiny section of the photosensitive surface of the opto-electrical converter, corresponding to the element $p(X, Y)$. After amplification the signal is changed by the electro-mechanical converter into the pressure of the needle on the skin of a blind person. Very small electromagnets with needles, or electrostrictive (piezoelectric) or magnetostrictive transducers are the operative elements. A relatively low resolution of the operative systems is the basic disadvantage of these aids. Their usefulness is also reduced by the elasticity of the skin.

The hearing aid has none of these faults. The resolution of the currently produced tiny integrated photodetector matrixes is over 150 000 elements of the screen. In the acoustical aid working in real time, the required resolution of the screen of the optoelectrical converter is $M \times N = 600 \times 20 = 12\,000$ elements. At the same time transformation of whole lines of the screen to sound permits a parallel, simultaneous analysis of whole lines by the hearing organ of a blind person. Further accelaration of the perception of the aid sounds is possible with a parallel analysis of the whole screen. Under a considerable simplification it can be assumed that a parallel analysis of information is usually performed by the right hemisphere [4], with the left hemisphere of the brain usually carrying out a serial data analysis. Thus the sound from the aid should be usually directed to the right hemisphere of a blind person's brain so as to permit the fastest perception of images, e.g. through placing the earphone at the left ear. It seems that a person who was born blind has the greatest possibility to learn to recognize quickly the optical images transformed into sound signals, up to the age of five. His right hemisphere of the brain — provided it is healthy — is fully capable of a parallel analysis of both sounds and images. The right hemisphere of a blind person who, however, lost sight later in his life, is specialized in understanding, particularly, of optical images [3, 4]. The sounds from the aid can be, however, analyzed through understanding, mainly through a serial analysis performed by the left hemisphere of the brain, already accustomed to the analysis of sounds [4, 3]. The understanding can be based on the equivalent transformation of an optical image to a spectral sound image, as presented in this paper. Some characteristics of optical images and most frequent scenes can in time be used as standards for a parallel analysis of sounds from the aid [6].

A blind person can in time become accustomed to some technical shortcomings of the aid [6], e.g. different sensitivities of individual photodetectors on the screen surface, optical distortions, and those due to the electronic elements of the aid.

Recognition of coloured images and increased contrast in images can be archived by the application of suitable optical filters. An increase in contrast in black and white images (and also coloured) can be attained electronically by the application of a method of the side effect of the vision [2].

The positions of objects are correctly determined relative to the body of a blind person if the opto-electrical converter is stiffly attached to the body

in the some manner each day; otherwise a blind person would have to "calibrate" the position of the artificial eye relative to the body.

Acknowledgement. I am grateful to Dr. R. GUBRYNOWICZ for essential help and instruction in preparation of this paper.

References

[1] A. CHORZEMPA, *Description of an attempt at using the touch for perception of human speech* (in Polish), Probl. Techn. Med., IV, 4 (1973).

[2] R. GAWROŃSKI, *Bionics* (in Polish), PWN, Warszawa 1970.

[3] K. JABŁONOWSKA, W. BUDOHOSKA, *Hemispheric differences in the visual analysis of the verbal and non-verbal material in children*, Acta Neurobiol. Exp. **36**, 693-701 (1976).

[4] K. JABŁONOWSKA, *Functional asymmetry of the brain in children with normal and retarded development of form perception* (in Polish), doctor thesis, Institute of Experimental Biology, Polish Academy of Sciences, Warszawa 1977.

[5] Z. KULKA, M. NADACHOWSKI, *Integrated linear systems and their application*, Atomic Energy Information Centre, 514, Warszawa 1973.

[6] E. KURCZ, *Private communication*, July 1978, Warszawa

[7] E. KURCZ, *Elektroftalm – a device for the blind* (in Polish), Elektronika **4**, 156-160 (1978).

[8] J. PIEŃKOS, J. TUCZYŃSKI, *Integrated* TTL *systems* (in Polish), WKŁ, Warszawa 1977, p. 289.

[9] M. A. SAPOZHKOV, *Speech signal in telecommunication and cybernetics*, Warszawa 1966 (translated from Russian).

[10] Z. M. WÓJCIK, *A mathematical model of determination of speech signal parameters using instant memory*, Archiwum Akustyki **2**, 121-137 (1977).

[11] Z. M. WÓJCIK, *The alignment of graphic images in solid-state technology*, Microelectronics and reliability **15**, 613-618 (1976).

[12] Z. M. WÓJCIK, *Operator for automatic detection of faults and compensation of distortion of graphic images* (in Polish), Archiwum Automatyki i Telemechaniki, 4, 455-471 (1977).

[13] E. ZWICKER, R. FELDKELLER, *Das Ohr als Nachrichtenempfänger*, S. Hirzel Verlag, Stuttgart 1967.

[14] R. L. GREGORY, *Eye and brain, Psychology of vision* (in Polish), PWN, Warszawa 1971.

[15] J. PIERCE, E. DAVID, *The world of sound* (in Polish), PWN, Warszawa 1967.

Received on June 18, 1978;
revised version on March 3, 1979

ARCHIVES OF ACOUSTICS
4, 4, 347-352 (1979)

IPSILATERAL STIMULUS INTENSITY AND TYMPANOMETRY IN MAN*

VED RAM SINGH

National Physical Laboratory
Hillside Road, New Delhi – 110 012 (INDIA)

The tympanometric characteristics of a human eardrum are studied under the influence of various intensities of the ipsilateral stimulation for the acoustic reflex. Emphasis is placed on the position of the tympanograms relative to atmospheric pressure, at the different stimulus intensities. The results indicate that there is no deviation of the notch of the tympanogram in the intensity range from 40 to 75 dB SPL, but there is an increase in the relative shift of the notch above 75 dB SPL. The change in deviation is caused by the suppression of the elicitation of the stapedius muscles in man. The ratio of the deviation, with and without the stimulus, is found to be 2.35 at 1000 Hz, 115 dB SPL, the highest intensity used in this work. The results reported are the average values of six normal human ears.

Introduction

Tympanometry which is one of the techniques of measuring the acoustic impedance of the ear, is gaining in importance [1, 4, 7-10, 15]. This technique assesses the mobility, or compliance, of the tympanic membrane during variation of the air pressure in a hermetically sealed ear canal. A tympanogram, which is a graph relating the change in compliance of the eardrum to the variation of air pressure in the ear canal, is generated by this technique. In other words, the tympanogram is a pressure compliance function. The observed or recorded change of the sound pressure level of the probe tone in the ear canal is an expression of the relative change of the impedance of the tympanic membrane and the middle ear. This change is expressed either in decibels or in cubic centimeters.

An electro-acoustic impedance bridge is generally used for tympanometry and intra-aural muscle reflex measurements [4,8]. A number of other measure-

* This investigation was carried out at the Mount Sinai Hospital in Toronto and the University of Toronto, Toronto (Canada).

ment techniques have been developed using the acoustic reflex as the basis of the test. These tests include estimation of the hearing loss using filtered white noise and, perhaps more importantly, using ipsilateral stimulation. Recently, Madsen Electronics Oakville, Ontario, Canada, has developed a modified version of the electro-acoustic impedance bridge with the facility of presenting an ipsilateral stimulus, in addition to the contralateral stimulus. The availability of this ipsilateral bridge has made the present investigation possible.

The aim of the present work is to study tympanometry in man at various intensities of ipsilateral stimulation. The position of the tympanograms with respect to atmospheric pressure is examined.

Material and method

Apparatus. The equipment used in this investigation consisted of an electro-acoustic impedance bridge (Madsen, ZO-72I) and a chart recorder. This bridge had a probe tone frequency of 220 Hz. Only two tones of 1000 Hz and 2000 Hz at intensities of 40 to 115 dB SPL were available in the instrument used for the presentation of ipsilateral stimulation with the probe tone. A tone of 1000 Hz at 40 to 115 dB SPL was selected for the present work.

Subjects. Three male subjects in the age range 20-30 years were examined. None of them could recall having suffered from any middle ear infection. The outer ear and the tympanic membrane had a normal appearance. Both of the ears of each person were used in this work.

Procedure. The *I/C* switch of the impedance bridge was kept at *I* for presentation of ipsilateral stimulation at 1000 Hz. Tympanograms were recorded at different hearing levels in the range 40 to 115 dB SPL. The air pressure control of the impedance bridge was adjusted to sweep smoothly through a pressure range from $-$ 200 to $+$ 200 mm (H_2O) in a period of 45 seconds. This unit monitors the actual changes in air pressure in the ear canal [16, 17]. The sensitivity of the graphic recorder was held constant for all measurements. The recorder speed was set to 5 mm/sec for each test.

Results

The tympanograms were obtained at various intensities of the ipsilateral stimulation for three male subjects. Table 1 shows the average results of the six normal ears. The deviation of the notch, i.e. peak of each tympanogram

relative to atmospheric pressure was examined at various stimulus intensities. It was found that there was no effect of the ipsilateral stimulus intensity on the tympanometry in the intensity range from 40 to 75 dB SPL. However, an increase in the deviation, was found beyond 75 dB SPL. The ratio of deviation with and without presentation of ipsilateral stimulus, was found to be 2.35 at 1000 Hz, 115 dB SPL, the highest stimulus intensity used in the present investigation.

Table 1. Position of the tympanograms relative to atmospheric pressure at different intensities of the ipsilateral stimulation

Ipsilateral stimulus intensity [dB]	Deviation from zero pressure [mm H_2O]	Ratio of deviation with and without stimulus
Without stimulus	−20	1.00
40-75	−20	1.00
80	−30	1.50
85	−32	1.60
90	−35	1.75
95	−37	1.85
100	−40	2.00
105	−42	2.10
110	−45	2.25
115	−47	2.35

Pure tone = 1000 Hz.

It was observed that the individual differences were great, but all the subjects showed results which demonstrated that the position of the notch of the tympanogram was affected, deviated or shifted, by the presentation of different intensities above 75 dB SPL. It was verified that this deviation in the tympanograms was not due to any inherent noise, delay or any other cause arising from the equipment used. Thus the results were due only to the physiological behaviour of the ear, as has been indicated by several other investigators [2, 11].

Discussion

The results in Table 1 indicate that the shift in the position of the tympanogram is due to the activity of the tympanic muscles. The activity of these muscles is not affected by the ipsilaterally presented stimulus up to an intensity of 75 dB SPL for a pure tone of 1000 Hz. However, above 75 dB SPL, the relative shift of the notch of the tympanograms indicates that the muscle activity is suppressed by the pressure variation in the middle ear. It may be mentioned here that at the peak (i.e. notch) of the tympanogram, the pressure in the ear

canal is the same as in the middle ear. At this point the eardrum has its maximum mobility [7]. As has been reported earlier [3, 13], the compliance of the eardrum is found to be decreased during acoustic stimulation which, in man, is due primarly to the effect of the stapedius reflex [14]. Our results agree well with these findings. The middle ear reflex (stapedius) contraction, is changed upon the application of an ipsilateral stimulus (above 75 dB SPL), which is thus responsible for the relative shift of the position of the notch of the tympanograms.

It is known that the acoustic reflex to pure tones occurs at a sensation level (SL) of approximately 85 dB in the average normal ear, but the reflex SL is reduced by the presence of loudness recruitment [3, 5, 6, 12]. This occurs because the reflex is apparently mediated by the loudness of the sound signal. In the normal ear, this loudness level is reached for pure tones at sensation levels of 70 to 100 dB [3]. In an ear with loudness recruitment, however, the loudness level required to elicit the reflex is reached at a much lower level above the impaired threshold. From Table 1, it is also clear that the ipsilateral stimulus is effective only above 75 dB SPL, in shifting the position of the tympanograms with respect to atmospheric pressure. Generally, the loudness level [12] for normal human beings is 75 dB SL. Thus, from the above, it is quite clear that an ipsilateral sound stimulus has an effect on the position of tympanograms only above a loudness level for pure tones corresponding to a sensation level of 75 dB.

Conclusion

The effect of varying intensity of ipsilateral stimulation for the acoustic reflex, on the tympanometric characteristics of human eardrums, has been studied. It has been found that there is no effect from ipsilateral stimulation in the intensity range from 40 to 75 dB SPL, on the position of the tympanograms relative to atmospheric pressure. An increase in the relative shift, caused by the suppression of the elicitation of the stapedius muscle has been found above 75 dB SPL. The average value of the ratio of the deviation, with and without the stimulus, has been found to be 2.35 at 1000 Hz, 115 dB SPL, the highest stimulus intensity used in this investigation.

References

[1] W. L. Creten, K.J. van Camp, *Transient and quasistatic tympanometry*, Scand. Audiol. **3**, 39-42 (1974).

[2] T. J. Fria, P.W. Alberti, *Personal communication*. Department of Otolaryngology, Mount Sinai Hospital, Toronto, Canada.

[3] O. Jepsen, *Middle-ear muscle reflexes in man*. in J. Jerger, *Modern developments in audiology*, Academic Press Inc. New York 1963, 193-239.

[4] J. JERGER, *Clinical experience with impedance audiometry*, Arch. Otolaryngol. **92**, 311-324 (1970).

[5] I. KLOCKHOFF, *Middle ear muscle reflexes in man. A Clinical and experimental study with special reference to diagnostic problems in hearing impairment*. Acta Otolaryng. Suppl. 164 (1961).

[6] L. LAMB, J. PETERSON, S. HANSEN, *Application of stapedius muscle reflex measures to the diagnosis of auditory problems*, Int. Aud. **7**, 188-199 (1968).

[7] G. LIDÉN, J. L. PETERSON, G. BJÖRKMAN, *Tympanometry*, Arch. Otolaryngol. **92**, 248-257 (1970).

[8] G. LIDÉN, G. BJÖRKMAN, J. L. PETERSON, *Clinical equipment for measurement of the middle ear reflexes and tympanometry*, J. Speech Hear. Disord. **37**, 100-112 (1972).

[9] G. LIDÉN, E. HARFORD, O. HALLEN, *Automatic tympanometry in clinical practice*, Audiology **13**, 126-139 (1974).

[10] G. LIDÉN, *Tympanometry for the diagnosis of ossicular disuption*, Arch. Otolaryngol. **99**, 23-29 (1974).

[11] P. MADSEN, G. PAY, *Personal communication*, Madsen Electronics, Oakville, Ontario, Canada.

[12] O. METZ, *Threshold of reflex contractions of muscles of middle ear and recruitment of loudness*, Arch. Otolaryng. **55**, 536-543 (1952).

[13] A.R. MØLLER, *The middle ear*, in J.V. TOBIAS, ed., *Foundations of modern auditory theory II*, Academic Press Inc., New York 1972.

[14] A.R. MØLLER, *Bilateral contraction of the tympanic muscles in man*, Ann. Otol. Rhinol. and Laryngol. 70, 735-752 (1961).

[15] J. L. PETERSON, G. LIDÉN, *Tympanometry in human temporal bones*, Arch. Otolaryngol. **92**, 258-266 (1970).

[16] K. TERKILDSEN, N.S. SCOTT, *An electroacoustic impedance measuring bridge for clinical use*, Arch. Otolaryngol. **72**, 339-346 (1960).

[17] K. TERKILDSEN, K. A. THOMSEN, *The influence of pressure variations on the impedance of the human eardrum*, J. Laryngol. 73, 409-418 (1959).

Received on October 27, 1978

ARCHIVES OF ACOUSTICS
4, 4, 353-358 (1979)

CLINICAL USE OF ULTRASONIC CW DOPPLER TECHNIQUE IN STOMATOLOGY

S. MAGNUS, G. PARDEMANN, CH. THIERFELDER, S. VOGEL

Humboldt-Universität zu Berlin, GDR

All methods used in stomatological practice for assessment of blood supply to the pulp require sensitivity testing. This, however, is not a reliable diagnostic method. Blood movement in the pulp can be detected directly by means of CW Doppler ultrasound. This technique, consequently, is an objective method which seems to be suitable for the above purpose, The author's approach to the problem has been theoretical, with the view to examining the suitability of the method and to establishing technical parameters of a stomatological Doppler device. Preliminary results so far obtained from the use of the ultrasonic Doppler technique in testing blood supply to the tooth are presented in this paper. Both advantages and disadvantages of the method are discussed.

Introduction

Determination of tooth vitality is essential to any planning of suitable dental therapy. Vitality depends on sufficient blood supply to the pulp and intact nervous function (HOFFMANN-AXTHELM [1]). Clinical detection of blood movement in the tooth and prediction, in this manner, of intact pulp function have not been possible, as yet. Thermal, electrical, and mechanical stimulation tests as well as exploratory trepanation are used by the authors to check "tooth vitality". However, such tooth sensitivity testing does not provide accurate information on pulp condition proper (cf. THIERFELDER et al. [4]). Different methods were used by THIERFELDER [5] to assess blood supply to the tooth (intravital arteriography, micro-angiography, fluorescence angiography, nuclear diagnostic blood volume measurement, ultrasound Doppler method). The conclusion he drew from his results was that the ultrasonic Doppler technique was the best applicable under practice conditions.

Measurements

While measurement of the cross-section averaged flow velocity in arterial and venous vessels is a well-known procedure, some difficulty has to be overcome for blood flow measurement in small vessels. The dental structures have grossly

different acoustic properties, such differences being sources of sizeable problems in the determination of blood supply to the pulp. Most of the commercially available Doppler blood flowmeters, therefore, are not adapted to stomatological applications.

The authors assumed the prevalence of unfavourable conditions in their attempt to figure out the parameters an ultrasonic Doppler device should have for stomatological use. Velocities of about 0.28 $cm \cdot s^{-1}$ may be expected to occur in pulp vessels, just as in arterioles [3]. The operating frequency required for the detection of such low velocities should be some 100 MHz which, however, could not be used because of extremely high absorption in tissue. The highest operating frequency is 10 MHz. In such a case, velocity components of 1.5 $cm \cdot s^{-1}$ in the direction of sound propagation are detectable, with the Doppler frequency being about 200 Hz. Good acoustic contact or coupling between ultrasonic probe and tooth cannot be achieved unless the probe is positioned at the dental neck. The difference between the mean sound velocities in the pulp ($1.54 \cdot 10^3$ $m \cdot s^{-1}$) and tooth ($4.45 \cdot 10^3$ $m \cdot s^{-1}$) is of sizeable magnitude, and so the angle obtainable between sound beam and vessel in the pulp is 80 degrees only, as may be seen from Fig. 1. Hence, blood flow velocities beyond

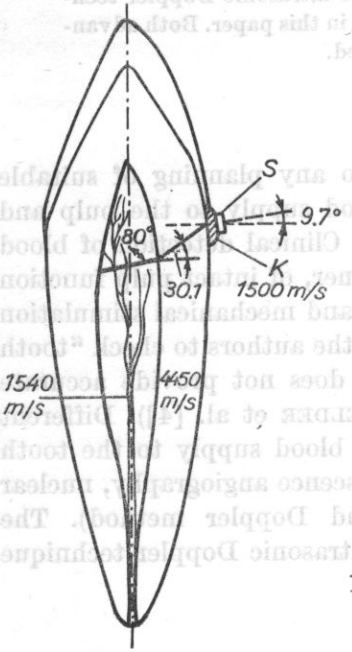

Fig. 1. Propagation of ultrasound beam in canine tooth diagram representation
S – ultrasonic probe; *K* – coupling gel

8.8 $cm \cdot s^{-1}$ will be detectable, and measurability will be reduced to the peak velocities during heart beat. Therefore, as shown in Fig. 2.2, the Doppler signal is likely to vanish, when marked change occurs to the blood vessels in the

pulp or to their elastic properties. Estimated losses along the pathway between transmitter and receiver are given in the level diagram.

Level diagram

Loss	dB
Transmitter crystal coupling	~ − 10
Reflections at tooth interfaces	~ − 20
Absorption	~ − 65
Backscattering	~ − 60
Receiver crystal coupling	~ − 10
total	~ −165

The estimated high-frequency transmitting power will be about 1 W, taking into account this special condition [4]. Preliminary experiments have shown that this value might be somewhat lower.

The potential benefits and shortcomings of the method should be summarised against the background of technical and clinical aspects.

Benefits

1. Convenient applicability to clinical practice, with no extraordinary preparations required.
2. No damage (observation of course of the disease).
3. Direct detection of movements due to blood stream in pulp.
4. With presence of fillings (amalgam, precious metal), no interference with or distortion of signal detection.
5. Objective nature of findings, no time-consuming evaluation.

Shortcomings

1. Very high sensitivity of device necessary.
2. Signal qualities so far obtainable are low.
3. Only peak velocities detectable in teeth.

Preliminary results

An ultrasonic Doppler device, Parks Model 806, has been used in preliminary clinical tests. Its power output is high and its operating frequency 9.5 MHz. The Doppler signals were received by earphone. The output voltages of the internal frequency-voltage converter were recorded on a signal-channel ECG recorder whereat the ds-components were lost. The dental status of a test person

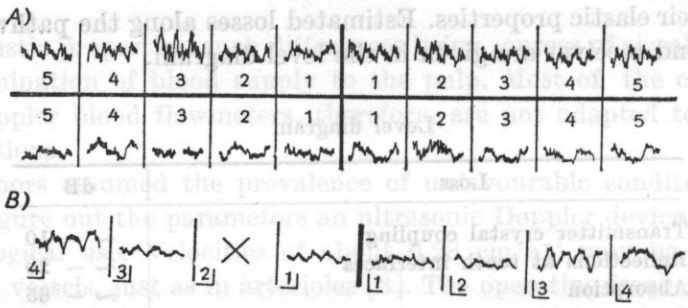

Fig. 2. Recordings of ultrasonic Doppler signals from tooth vessels
A – dental status of patient aged 20; *B* – dental status of patient between 14 and 24, following loss of twelve after orthodontic treatment

aged 20 is shown in Fig. 2A. Signal curves are reproducible and typical of each of the teeth. The curves obtained from the sides of the upper and lower jaws are comparable with each other, if none of the teeth is pathologically changed. It should be noted that the premolars in the upper jaw have two peaks (two root canals), while the intact canine teeth have high signal amplitudes. An

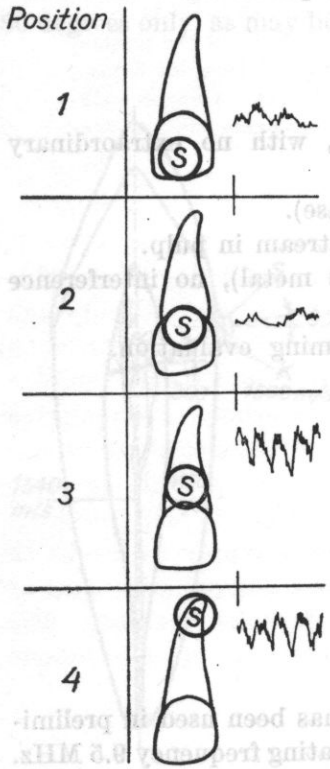

Fig. 3. Positions of ultrasonic probe relative to tooth
S – ultrasonic probe

atlas giving the curves of vessels in the pulp may be readily drawn. Figure 3 shows the positions of the ultrasonic probe relative to the tooth, with position 3 being preferred. An improved Doppler signal curve will be obtainable, if the

ultrasonic probe is used to compress without troubling the patient's gingiva (see Fig. 4).

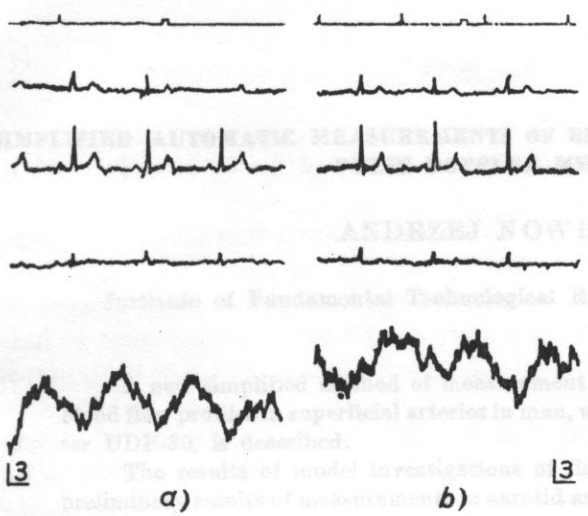

Fig. 4. Improvement of Doppler tracings with gingiva compressed by ultrasonic probe
a – gingiva compressed; *b* – gingiva not compressed

Conclusions

The CW ultrasonic Doppler method can be used to test dental vitality. Being applicable to clinical practice and provided some technical improvement, it can replace all sensitivity tests used in the past. Only qualitative results so far have been obtainable to this date. However, quantitative results may be expected, following technical improvement. A stomatological CW Doppler unit is now being developed and ultrasonic probes designed for the purpose by the authors in cooperation with "Manfred von Ardenne" Research Institute, Dresden, GDR.

References

[1] W. Hoffmann-Axthelm, *Zahnärztliches Lexicon*, 4th edition, Johann Ambrosius Barth Verlag, Leipzig 1964.

[2] S. Lees, F.E. Barbar, *Looking into teeth with ultrasound*, Science **161**, 477-478 (1968).

[3] H. Rein, M. Schneider, *Physiologie des Menschen*, 13th/14th editions, Springer Verlag, Berlin-Göttingen-Heidelberg 1960.

[4] Ch. Thierfelder, S. Magnus, G. Pardemann, S. Vogel, *Gefässfunktionsdiagnostik der Pulpa dentis – ein neues Anwendungsfeld des Ultraschall-Doppler-Verfahrens*, das Deutsche Gesundheitswesen, **33**, 24, 1105-1109 (1978).

[5] Ch. Thierfelder, *Die Blutversorgung des Zahnes – eine experimentelle Studie*, Medical dissertation "B", Humboldt Universität, Berlin 1978.

Received on November 20, 1978

ARCHIVES OF ACOUSTICS
4, 4, 359-366 (1979)

SIMPLIFIED AUTOMATIC MEASUREMENTS OF BLOOD FLOW BY THE ULTRASONIC PULSE DOPPLER METHOD

ANDRZEJ NOWICKI

Institute of Fundamental Technological Research (00-049 Warsaw)

A new simplified method of measurement and recording of time averaged blood flow profiles in superficial arteries in man, using an ultrasonic pulse flowmeter UDP-30, is described.

The results of model investigations of flows in tubes, and subsequently preliminary results of measurements in carotid and femoral arteries are discussed.

1. Introduction

Of all noninvasive methods for diagnosis on the circulation system, the ultrasonic pulse Doppler method is particularly noteworthy. At present, four devices of this type are produced in the world: Mark I by ATL, United States, Mavis by GEC-Medical, Great Britain, Echovar Doppler Pulsée by Alvar Electronic, France, and UDP-30 by ZD "Techpan" in Poland. One should mention the large number of laboratory devices being developed in many renowned scientific and research centres. This requires development of practical — and convenient in clinical use — measuring and recording methods and their adequate and inambigous interpretation.

2. The principle of automatic measurement of flow profiles

The principle of the pulse Doppler blood flowmeter was described in [3] where it was shown that knowing the angle θ between the direction of an ultrasonic beam and a blood vessel, the diameter of the vessel investigated and the blood flow velocity profile can be determined. The diameter can be expressed by the formula

$$d = \frac{ct}{2} \sin\theta, \tag{1}$$

where t is the arrival time between the front and the rear walls of a blood vessel, c — the ultrasound propagation velocity in blood (≈ 1550 m/s). The blood flow velocity can be determined from the formula

$$V = \frac{f_d c}{2 f_n \cos\theta}, \tag{2}$$

where f_d is Doppler frequency equal to the difference between the frequency of a transmitted signal and that of a signal scattered by blood cells, and f_n is the transmitted signal frequency.

Both the vessel diameter and the flow velocity are a function of the angle θ which is usually unknown. It is relatively easy to determine the angle θ for vessels directly under the skin and parallel to the skin plane. With respect to the deeper vessels it is necessary to use a more complicated measurement technique, using a special double-transducer head permitting the angle θ to be determined by way of triangulation [1].

Most pulse Doppler blood flowmeters are equipped with an electronic analyzing gate with an adjustible delay time relative to the transmitted pulse [3]. Thus the measurement of the flow velocity profiles and the vessel diameter can be taken by a manual adjustment of the analyzing gate delay.

The technique for measurement of flow profiles, using the abovementioned devices, and the calculation of the blood flow rate from profiles obtained are time consuming, making complex clinical measurements difficult sometimes; in particular, during operations.

The automatic shift of the analyzing gate across the vessel investigated to a great extent accelerates the investigation and the recording of results [4].

With an automatic, directly adjustible delay of the analyzing gate B, the distribution of the curve for the blood flow velocity (averaged in time) from the velocity 0 at the front vessel wall through the maximum volocities in the center of the vessel to again the velocity 0 at the rear wall, is shown on the recorder paper tape (Fig. 1). Knowing the velocity u_1 of the automatic delay of the analyzing gate B, the speed u_2 of the paper tape shift, and lengths of the sections S_1 and S_2 between the zero flow values for the transducers P_1 and P_2, respectively, the vessel diameter can be determined from the formula

$$d = \frac{u_1}{u_2} S_1 \sin\theta, \tag{3}$$

where

$$\theta = \frac{\varphi}{2} + \tan^{-1}\left(\frac{S_2 - S_1}{S_2 + S_1} \tan\frac{\varphi}{2}\right), \tag{4}$$

φ being the angle between the transducers P_1 and P_2.

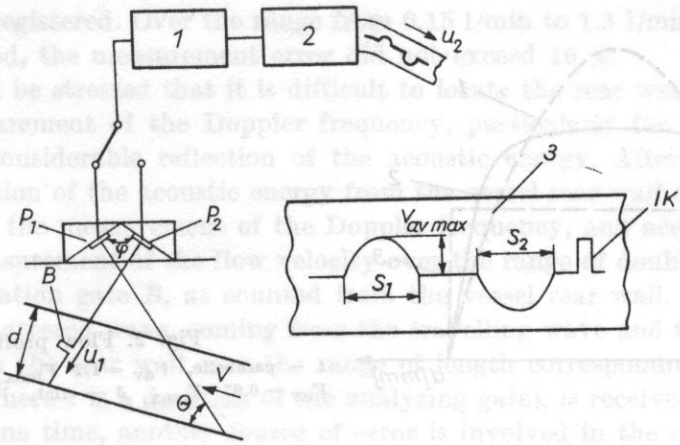

Fig. 1. The principle of automatic blood flow measurement

1 – ultrasonic pulse Doppler flowmeter, *2* – recorder, *P1*, *P2* – ultrasonic transducers, *B* – analyzing gate, u_1 – automatic delay velocity of analyzing gate, u_2 – shift velocity of recorder tape, *3* – recording of time averaged profiles of blood flow velocity obtained by means of an ultrasonic beam produced by transducers P_1 and P_2 respectively, *IK* – calibration impulse

In the case of operational investigations, the angle θ between the ultrasonic beam and the vessel is known, and for the heads used it equals 67°. For such an angle expression (3) takes the form

$$d = 0.91 \frac{u_1}{u_2} S_1. \tag{5}$$

The device is equipped with a system for recording a standard Doppler signal (the so-called calibration impulse *IK*), the amplitude of which corresponds to the Doppler frequency $f_{dK} = 1000$ Hz. For $\theta = 67°$ the calibration impulse amplitude corresponds to the standard calibration velocity $V_K = 30$ cm/s. Knowing the magnitude of the calibration impulse, the maximum mean (time averaged) velocity amplitude of blood flow, $\overline{V}_{max}$ can be read from the recorder paper tape. Accordingly, the blood flow rate is defined by the formula

$$Q = 0.67\, \overline{V}_{max} \frac{\pi d^2}{2}. \tag{6}$$

The numerical coefficient 0.67 in (6) has been obtained experimentally for carotid and femoral arteries by comparison of time averaged flow profiles measured using the above method with the distribution of instantaneous profiles. Introduction of this coefficient can also be justified physically, the blood flow profile in vessels usually being neither parabolic nor flat but lying between the two (Fig. 2). In the case of laminar flow (parabolic profile) the mean flow velocity is equal to half its maximum value. For turbulent flow the profile becomes considerably flattened so that the mean velocity value nears its maximum value.

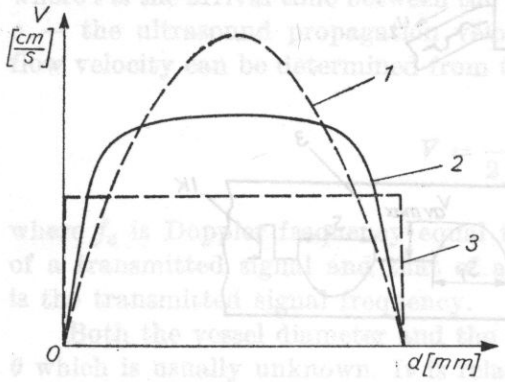

Fig. 2. Flow profiles
1 – parabolic, $V_{av} = 1/2\ V_{max}$, *2* – flattened, $V_{av} = 0.67\ V_{max}$, *3* – flat, $V_{av} = V_{max}$

Experimental investigations were carried out *in vitro* on a laboratory model, assuming a stationary liquid flow in a plexiglass tube with a diameter $d = 8$ mm and length $l = 100$ cm.

Starch suspension in a mixture of distilled water and glycerine at the ratio of 100 g starch to 10 l liquid was used. The kinematic viscosity of the mixture was equal to $2.2 \cdot 10^{-2}$ St. The flow in the velocity range corresponding to the Reynolds number of 200 to 1700, i.e. in the range of laminar flow, was inve stigated. Selected measurement results are shown in Fig. 3.

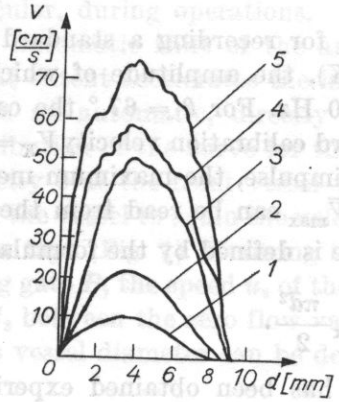

Fig. 3. Flow profiles recorded for various rates Q
1 – $Q = 0.15$ l/min., *2* – $Q = 0.4$ l/min., *3* – $Q = 1$ l/min., *4* – $Q = 1.2$ l/min., *5* – $Q = 1.4$ l/min.

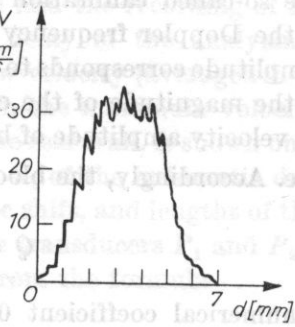

Fig. 4. An example of time averaged flow profile recorded for the external carotid artery

The results obtained were verified against the actual flows in the tube, comparing the flow rates determined by measuring the volume of a liquid flowing out of the tube in a time unit with the flow rates calculated from the

flow profiles registered. Over the range from 0.15 l/min to 1.5 l/min of the flow rates measured, the measurement error did not exceed 10 %.

It should be stressed that it is difficult to locate the rear wall of the tube by the measurement of the Doppler frequency, particularly for tubes whose walls cause considerable reflection of the acoustic energy. After JORGENSEN [2] the reflection of the acoustic energy from the vessel rear wall can influence the results of the measurement of the Doppler frequency, and accordingly the results of measurement of the flow velocity over the range of double the length of the observation gate B, as counted from the vessel rear wall. Because the energy of a scattered wave, coming from the travelling wave and from the one reflected from the rear wall over the range of length corresponding to a time interval 2τ (where τ is a duration of the analyzing gate), is received by a receiver at the same time, another source of error is involved in the measurement of the Doppler frequency. In the case of blood vessels, the effect is usually very small, because the reflection of the acoustic energy from the boundary of the vessel wall and tissue is slight due to close values of respective acoustic impedances.

3. Measurements of blood flow in carotid and femoral arteries in man

Preliminary investigations of the method were carried out, measuring the flow in the external carotid artery in seven healthy young men. The diameters of vessels measured ranged from 6 to 7 mm and flow rates calculated from formula (6) ranged from 0.2 l/min to 0.25 l/min. These results also agree with the generally accepted values of physiological flows. They also agree with the results of measurement of blood flow in a common carotid artery, ranging from 0.35 l/min to 0.5 l/min under the assumption of twice as much blood flowing in the artery, compared to the internal or external carotid arteries [1,4].

Figs. 5a and 5b show examples of flows recorded in the common carotid and superficial femoral arteries in a healthy man (J.K., aged 57). The vessel diameters measured were 6 mm for the carotid artery and 6.5 mm for the femoral artery, and the flow rates calculated were 0.38 l/min. and 0.24 l/min. respectively. The recordings in Figs. 5a, b — *1*, *2* show curves for instantaneous and mean velocities, respectively, measured in the vessel center (fixed analyzing gate).

The recordings in Figs. 5a, b — *3*, *4* show distributions of instantaneous and mean velocities across the vessel with an automatically shifting analyzing gate. The shape of recordings obtained for the mean velocity distribution (Fig. 5, a, b — *4*) is irregular, particularly for the femoral artery where the flow pulsation effect was not sufficiently filtered This would suggest insufficient efficiency of the filter which averages the signal proportional to the blood flow velocity However, an increase in the filter time constant would greatly distort

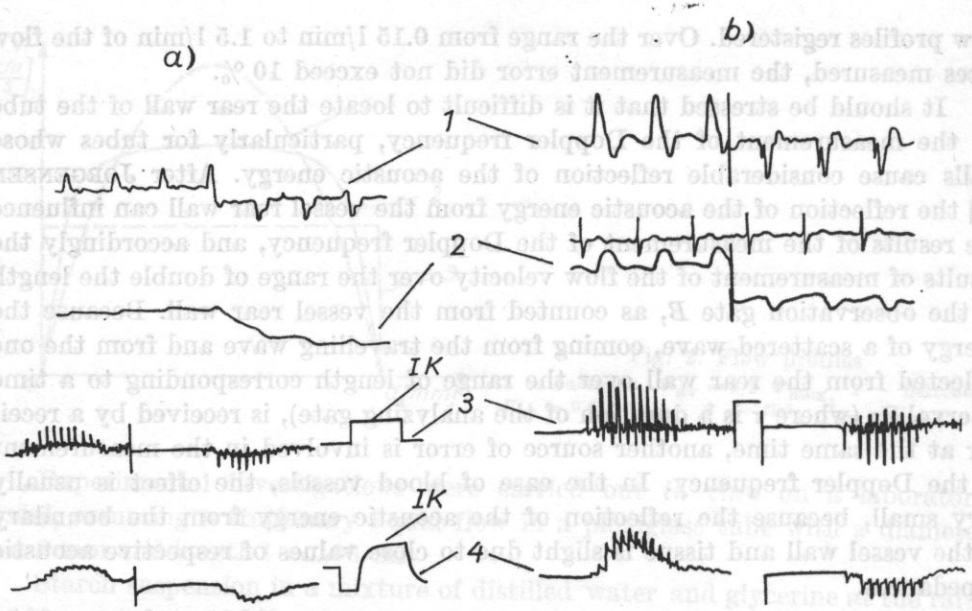

Fig. 5. Flow velocities recorded for (a) carotid artery and (b) femoral artery
1 – instantaneous flow velocities in the vessel centre, *2* – mean flow velocities in the vessel centre, *3* – instantaneous flow velocity profiles, *IK* – calibration pulses

the registered profile, particularly for the vessel front and back walls (long rise and drop times for a flitered signal). Expressed in the asymmetry of the profile relative to the vessel center, this effect is already visible in the currently used filter with a time constant of 3 s. The effect of the filter is also seen in the fuzzy profile contour, particularly at the real wall. Therefore, a more exact measurement of the vessel diameter is obtained, taking into consideration the recording lengths (S_1 and S_2 in Fig. 1) for the instantaneous velocity distribution (Figs. 5a, b – *3*).

4. Conclusions

The present method, although it accelerates the recording and interpretation of measurements of the blood volume flow, in the case of measurements in vivo can introduce the measurement error of about 30 %, which results from the shape of the time averaged flow profile (cf. Fig. 2), accepted under a simplified assumption. This error seems small for large vessels with a diameter larger than 5 mm. For small vessels with diameters of 2 to 3 mm, the flow profile is usually very much flattened, and accordingly the blood flow rates calculated from formula (6) will be underrated. It seems that the main advantage of the method is a direct recording of the vessel diameter on the recorder paper tape, permitting an easy estimation of the obstruction degree and a direct comparison of the vessel diameters before and after removal of the obstruction.

References

[1] K. Borodziński, L. Filipczyński, A. Nowicki, T. Powałowski, *Quantitative transcutaneous measurements of blood flow in carotid artery by means of pulse and continuous wave Doppler methods*, Ultrasound in Medicine and Biology **2**, 189-193 (1976).

[2] J. E. Jorgensen, D. N. Campau, D. W. Baker, *Physical characteristic and mathematical modelling of pulse ultrasonic flowmeter*, Med. and Biol. Engng. **12**, 4, 404-420 (1973).

[3] A. Nowicki, *Ultrasonic pulse Doppler method in blood flow measurement*, Archives of Acoustics **2**, 4, 305-323 (1977).

[4] A. Nowicki, *Automatic simplified measurement of blood flow by means of ultrasonic pulse Doppler method*, Digest of papers of 1st Mediterranean Conf. on Med. and Biol. Engng., Vol. 1, 4-17, September 12-17, Sorrento 1977.

Received on December 19, 1978

8TH WINTER SCHOOL OF QUANTUM AND MOLECULAR ACOUSTICS, AND SONOCHEMISTRY

USTROŃ - JASZOWIEC 1979

A successive Winter Shool of Quantum and Molecular Acoustics, and Sonochemistry took place in Ustroń-Jaszowiec on March 5-10, 1979. It was organized under the interdepartmental problem MR. I. 24 by the Higher Silesian Division of Polish Acoustical Society, Physics Institute of Silesian Technical University, Gliwice, and Institute of Fundamental Technological Research, Warsaw. The School was attended by 100 persons from 10 scientific centres.

Compared to previous years, both the number of the attendess of the School and that of contributed papers were considerably greater. Therefore, in addition to plenary papers and reports on authors own investigations, round-table sessions and poster form presentation of some papers, were introduced. Discussions took place in form of 6 sesions where 55 papers and communiqués deroted to the current state of investigations in the fields of quantum and molecular acoustics, acoustoelectronics and acoustooptics, sonochemistry and ultrasonic spectroscopy were presented.

Special attention should be paid to the increased interest in acoustooptics and integrated optics, whose expression were round-table sessions devoted to these subjects. The school attendees were given printed materials from the last year's School, which enabled them to see more thoroughly the progress in the investigations being carried out.

On the 4th day of School the IIIth plenary session of the section of Molecular and Quantum Acoustics of Polish Acoustical Society was held, chaired by prof. dr Z. Jagodziński, vice-chairman of Executive Board of Polish Acoustical Society. The president of the Executive Board of the section, prof. dr A. Opilski reported on the activities of the section, and the perfomance of the Executive Board was unanimousky accepted by vote. Subsequently, prof. dr Z. Jagodziński in warm words thanked the outgoing Executive board and its Chairman, in particular, for the large contribution they had made to the organization of work of the section and the School.

In the election, a new Executive Board was established including: chairman — prof. dr hab. A. Śliwiński (Physics Institute, Gdańsk University), vice-chairman — prof. dr hab. A. Opilski (Physics Institute, Silesian Technical University, Gliwice), secretary — dr A. Markiewicz (Physics Institute, Gdańsk University), members — dr M. M. Dobrzański (Institute of Fundamental Technological Research, of the Polish Academy of Sciences, Warszawa) and dr A. Juszkiewicz (Chemistry Institute, Jagiellonian University).

During lively discussion, a number of problems concerning both the work plan and a future form of the School were considered, closer cooperation of the School with the Coordinator of the Interdepartmental Problem MR.I.24 and, in particular, in the elaboration of a draft for the next five-year plan, were postulated. The need for production of a shorf series of ultrasonic spectrographic apparatus was pointed out. Most speeches concerning the School centred on the possibilities of inviting outstanding foreign experts and expanding the scope of native lecturers. Round-table discussion and poster form presentation were appreciated as a valuable introduction.

The papers chosen by the Scientific Committee from papers delivered, will be published in a book, as last year.

The informal evaluation of the organization of the School, interpersonal contacts and coordination of research, was presented in couplets, at the general get-together meeting. Discussion in the lobby permitted the exchange of views between the representatives of narrow fields of interest, for one should not forget the interdisciplinary character of acoustics which often caused the temperature of discussion to rise (problems related to quantum bioacoustics, spectroscopy and T. Jefferson effect can be mentioned as examples).

Although the weather was not very good, but the atmosphere of warm and understanding created by the Organizational Committee made discussions nice and contributed to closer intellectual contacts between representatives of different research centres, for which acknowledgement is due to the organizers: prof. dr hab. A. OPILSKI – director of Physics Institue, Silesian Technical University, Gliwice; dr Z. KLESZCZEWSKI – president of High-Silesian Division of Polish Acoustical Society, the ever-smiling Mrs B. KOCHOWSKA – organization secretary of the School, and dr J. BERDOWSKI.

Plenary papers

1. J. FINAK, H. JEROMINEK, *Selected methods for investigation of properties of planar fibrescopes used in integrated acoustoptics.*
2. Z. KLESZCZEWSKI, *Practical application of interaction of laser light and bulk acoustic waves.*
3. W. PAJEWSKI, *Generation, propagation, and detection of BG transverse surface waves.*
4. B. PASZKOWSKI, *New technologies in microelectronics. Integrated optics.*

Reports on individual research

5. M. ALEKSIEJUK, *Parameters of tunnel junctions used to generate and detect hypersonic vibrations.*
6. Z. BARTYNOWSKA, A. JUSZKIEWICZ: *Physical and chemical characteristics of rotation transitions occurring in esters from measurements of damping and velocity of ultrasonic waves.*
7. J. BERDOWSKI, M. STROZIK, *Heterodyne and diffraction methods for detection and visualization of surface acoustic waves.*
8. M. BŁACHUT, *Damping of surface waves in dielectrics at high temperatures.*
9. A. BYSZEWSKI, *Changes in optical properties of a crystal, caused by a surface acoustic waves.*
10. Z. CEROWSKI, J. KAPRYAN, *Measurements of the acoustoelectrical effect in a piezoelectric – semiconductor layer system.*
11. M. M. DOBRZAŃSKI, *Relation between de Broglie's theory and quantum representation of hypersonic wave.*
12. A. DROBNIK, *Generation of mechanical waves by laser light beams*
13. A. DRZEWIECKA, *Visualization of mechanical waves using the stroboscopic method.*
14. A. FILIPCZYŃSKA, *Propagation of an acoustic wave along a hollow cylinder immersed in a liquid.*
15. J. FILIPIAK, *Surface acoustic waves spectrum analyser*
16. J. FRYDRYCHOWICZ, *On a new possibility in the field of X-ray analysis of crystal lattice dynamics.*
17. J. GMYREK, K. WANAT, *Determination of thermodynamic constants of a liquid by the acoustic method.*
18. A. GRZEGORCZYK, A. JUSZKIEWICZ, *Investigation of relaxation processes in the isotropic phase of p-alcoxybenzoic acids by ultrasonic methods.*
19. Z. JAKUBCZYK, A. KRZESIŃSKI, *Measurement of propagation parameters of surface acoustic waves in the* ZnO*-glass layer system.*

20. Z. KACZKOWSKI, *The effect of magnitic polarization on ultrasound velocity in alfer 33 kHz band transducers.*

21. Z. KLESZCZEWSKI, A. MLECZKO, *Interaction of acoustic waves and high intensity laser light.*

22. Z. KOZŁOWSKI, A. JUSZKIEWICZ, J. KOPYŁOWICZ, *Measurements of some anomalies in ultrasonic waves propagation in water.*

23. J. KRZAK, F. KUCZERA, *On a common mistake made in evaluation of intermolecular interaction in liquids.*

24. P. KWIEK, *Optical impulse holography used to investigate ultrasonic fields.*

25. P. KWIEK, P. CZYŻ, A. MARKIEWICZ, *Investigation of ultrasonic field distribution from reproduced time averaged holograms of the field.*

26. P. KWIEK, A. ŚLIWIŃSKI, *The optical hologram of a travelling ultrasonic wave.*

27. H. LASOTA, *Problems in radiation of acoustic sources in infinite baffles.*

28. Cz. LEWA, *Criteria for evaluation of the existence of rotation phase transitions in liquids.*

29. P. LORANC, *X-ray investigation of piezoelectric monocrystal $LiIO_3$ transducers.*

30. M. ŁABOWSKI, *Experimental determination of mean relaxation time for concentration fluctuation in selected critical mixtures.*

31. P. MIECZNIK, *Investigation of structure stability in water solutions of hexamethyphosphorotriamide by the acoustic method.*

32. A. OPILSKI, M. URBAŃCZYK, *Acoustic impedance of an isotropic medium for a surface wave.*

33. J. OSTROWSKI, *Lithography methods in the planar technology of optoacoustic elements.*

34. R. PŁOWIEC, *Representation of viscoelastic relaxation range in some electrolytes by the Lamb liquid model.*

35. R. RESPONDOWSKI, F. KUCZERA, *On some molecular and thermodynamic problems in propagation of acoustic waves in liquids under high pressure.*

36. H. RYLL-NARDZEWSKA, J. RANACHOWSKI, K. KUNERT, *Ultrasonic investigation of cross-linked polyethylene.*

37. B. SIKORA, *Methods of measurement by a focussed ultrasonic beam in a solid.*

38. W. SZACHNOWSKI, *Damping measurements in oil-solid type mixtures.*

39. M. SZALEWSKI, *Investigation of properties of thin-layer surface acoustic wave waveguides.*

40. J. TABIN, *Measurements of grain composition in crystal suspension by the echo method.*

41. Z. TYLCZYŃSKI, *Determination of piezoelectric and elastic properties of ferro-electric plane of TGS crystals.*

42. B. WIŚLICKI, *Viscoelastic properties of oils at kHz frequencies.*

43. B. ZAPIÓR, *The survey of accomplishments of the Sonochemistry Unit of Jagiellonian University.*

44. J. ZIENIUK, *Optically addressed ultrasonic transducers.*

Poster form papers

45. S. ERNST, R. PŁOWIEC, M. WACIŃSKI, *Investigation of viscoelastic properties of electrolytes in polyhydric alcohols.*

46. J. GLIŃSKI, *Sound velocity in some water-amine mixtures.*

47. A. GRZEGORCZYK, *Investigation of relaxation proccesses in selected liquid crystal substances near the nematic-isotropic liquid phase transition, using acoustic methods.*

48. A. KIDAWA, M. NOWAK, *Investigation of polycrystalline SbSJ.*

49. M. KRZESIŃSKA, A. KRZESIŃSKI, A. KWAŚNIEWSKA, *Investigation of hypersonic wave propagation in solids.*

50. W. LARECKI, *The influence of statistical deformation on the nonlinear effect accompanying propagation of finite amplitude acoustic wave.*

51. R. Leć, Cz. Gonzales, Z. Kozłowski, *Measurement of velocity and damping of ultrasonic waves in water saccharose solutions.*

52. M. Zwiernik, *An acoustic steam-supplied flow generator.*

53. K. Wanat, *Thermodynamic properties of stiff balls liquid model.*

54. M. Wojtkowiak, *Measurements of ultrasonic field in stell, using an electrodynamic probe.*

Round-table discussion

Achievements, development prospects and industrial application of acousto-optics.

M. M. Dobrzański (*Warszawa*)